

Astrophysical Objects

Active Galaxies

Based on: An introduction to modern Astrophysics chapter 28

Helga Dénés 2023 S2 Yachay Tech
hdenes@yachaytech.edu.ec



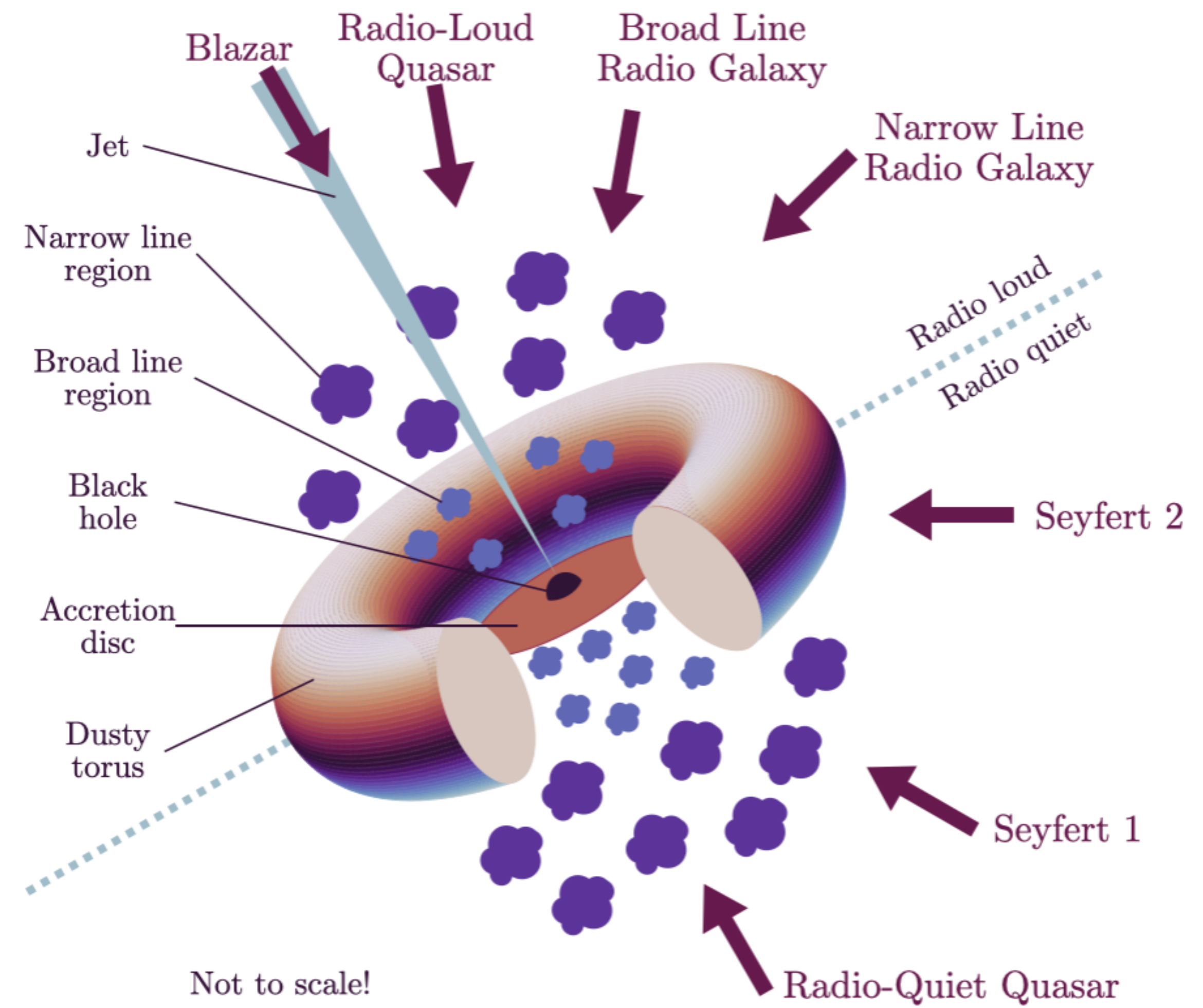
**SCHOOL OF
PHYSICAL SCIENCES
AND NANOTECHNOLOGY**

The unified model of AGN

Unified model of AGN adapted from Urry & Padovani (1995).

The thick arrows represent different viewing angles, and the observed object which results from them.

Note the asymmetry of the diagram; this is to demonstrate the two different possibilities of radio loud/quiet and is not representative of a single object.



Seyfert galaxies

NGC 1068

Edward A. Fath (1880– 1959), who in 1908 was observing the spectra of “**spiral nebulae**.”

Although most showed an absorption-line spectrum produced by the combined light of the galaxy’s stars, NGC 1068 displayed six **bright emission lines**.

In 1926 Edwin Hubble recorded the emission lines of this and two other galaxies.

Seventeen years later Carl K. Seyfert (1911–1960) reported that **a small percentage of galaxies have very bright nuclei** that are the source of **broad emission lines** produced by atoms in a **wide range of ionization states**. These nuclei are nearly stellar in appearance.



Seyfert galaxies

Today these objects are known as **Seyfert galaxies**, with spectra that are categorized into one of two classes. **Seyfert 1** galaxies have **very broad emission lines** that include both allowed lines (H I, He I, He II) and narrower forbidden lines (such as [O III]). Seyfert 1 galaxies generally have “narrow” allowed lines as well, although even the narrow lines are broad compared to the spectral lines exhibited by normal galaxies. The width of the lines is attributed to **Doppler broadening**, indicating that the allowed lines originate from sources with **speeds typically between 1000 and 5000 km s⁻¹**, while the forbidden lines correspond to speeds of around 500 km s⁻¹.

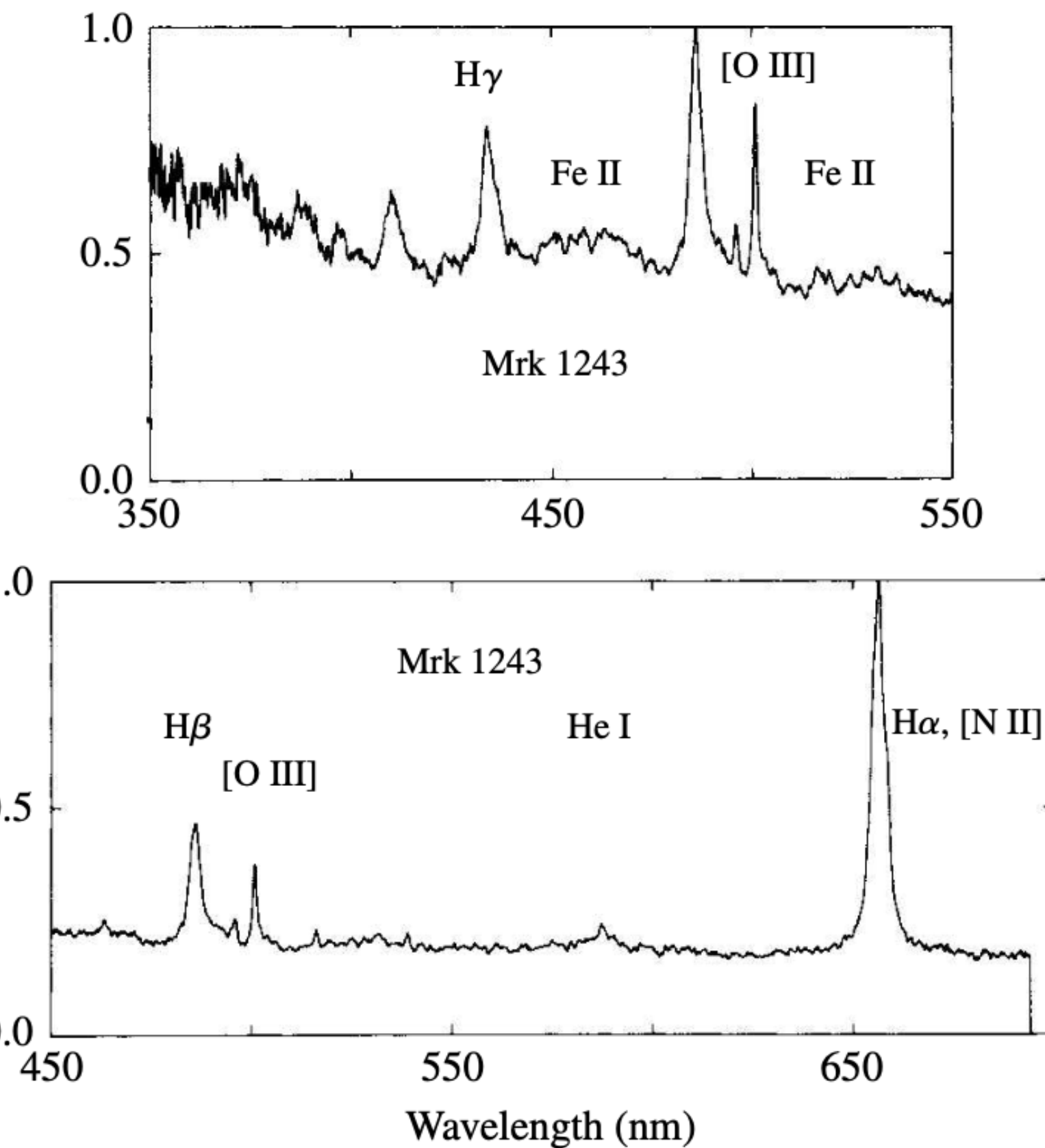


FIGURE 1 The visible spectrum of Mrk 1243, a Seyfert 1 galaxy. (Figure adapted from Osterbrock, *QJRAS*, 25, 1, 1984.)

Seyfert galaxies

Mrk 1243 - PanSTARS image

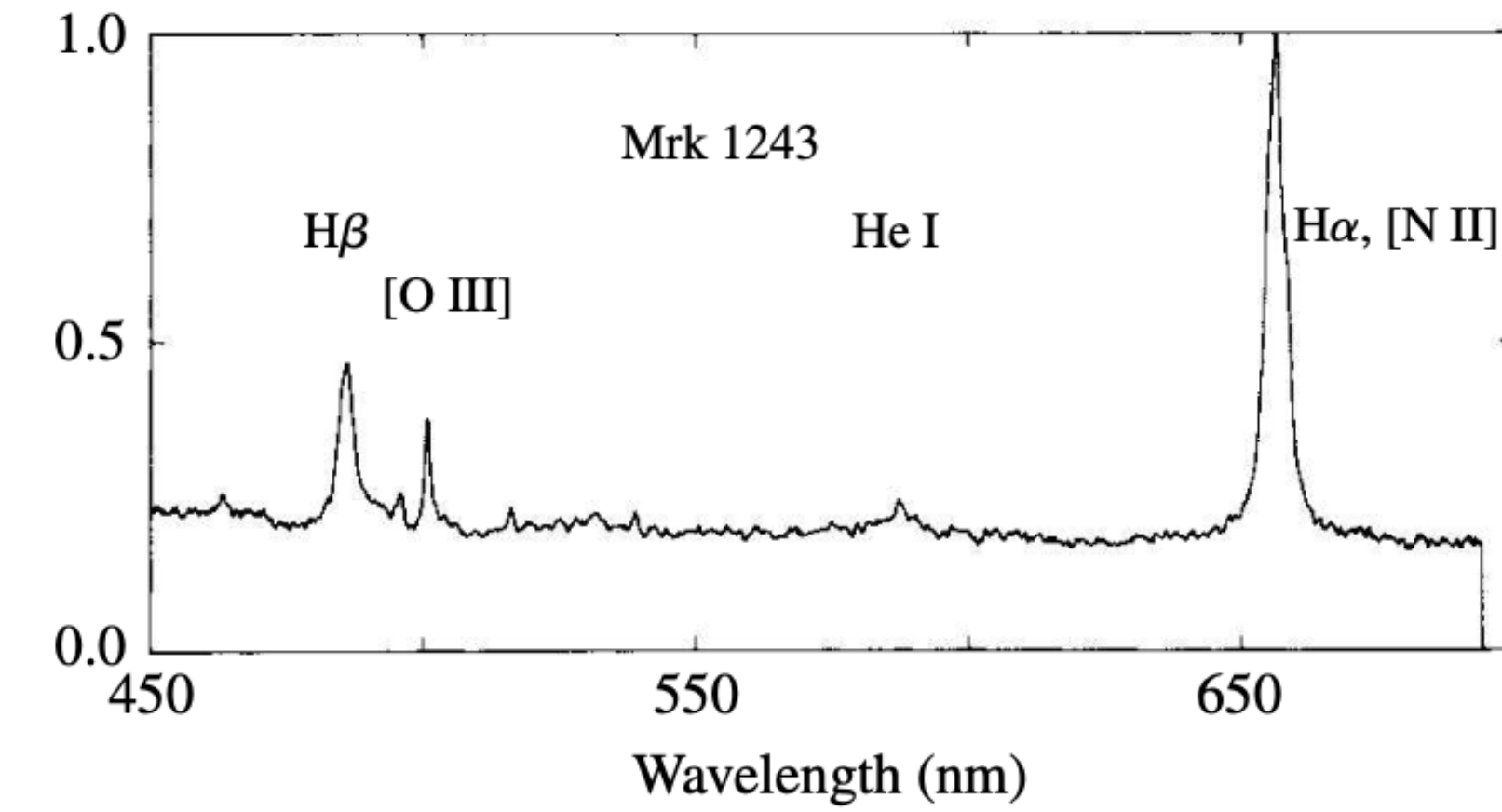
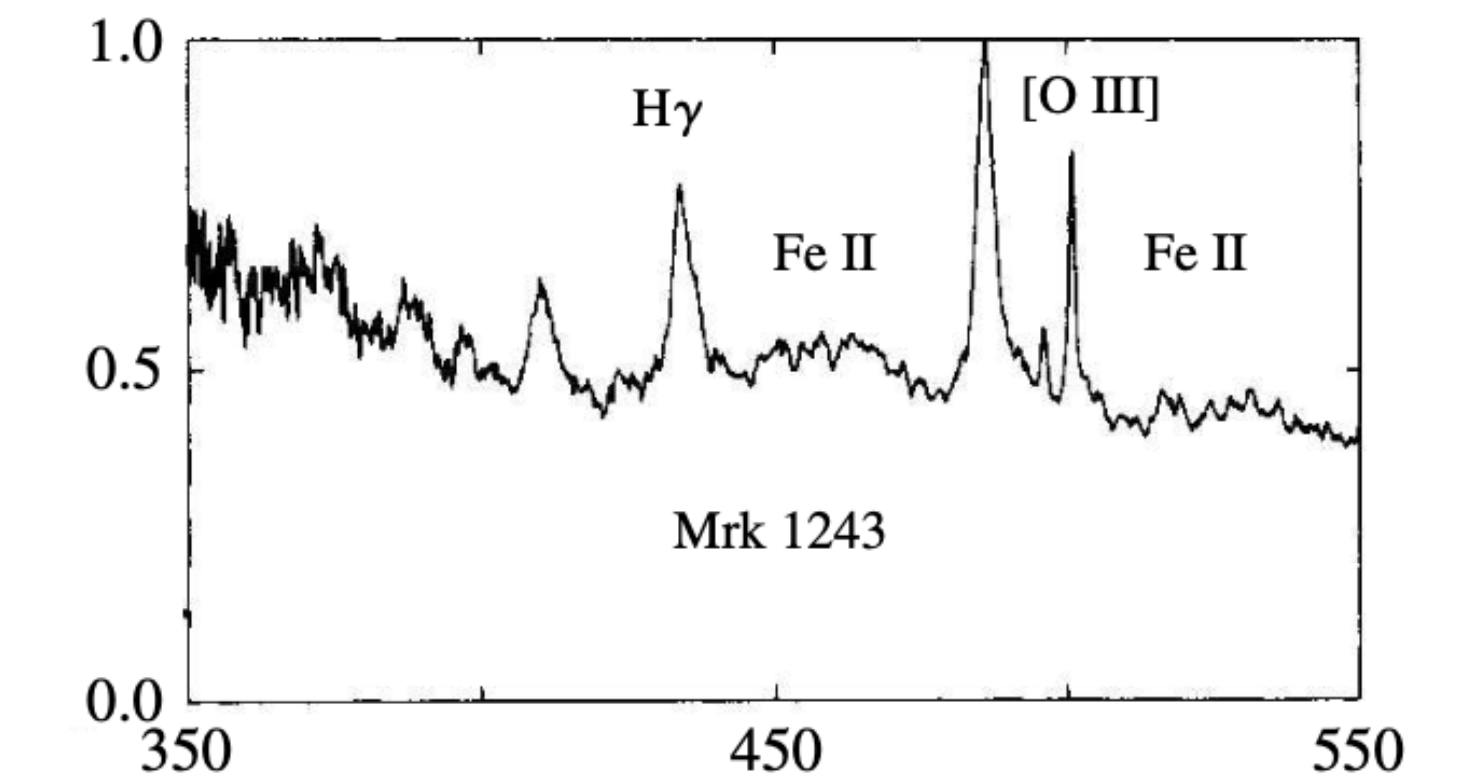


FIGURE 1 The visible spectrum of Mrk 1243, a Seyfert 1 galaxy. (Figure adapted from Osterbrock, *QJRAS*, 25, 1, 1984.)

Seyfert galaxies

Seyfert 2 galaxies have **only narrow lines** (both permitted and forbidden), with characteristic **speeds of about 500 km s⁻¹**. Every spectrum also shows a **featureless continuum** that is devoid of lines, originating from a small central source. The **great luminosity** of a Seyfert 1 galaxy arises from this continuum, which often overwhelms the combined light of all of the galaxy's stars. The continuum observed for a Seyfert 2 is significantly less luminous.

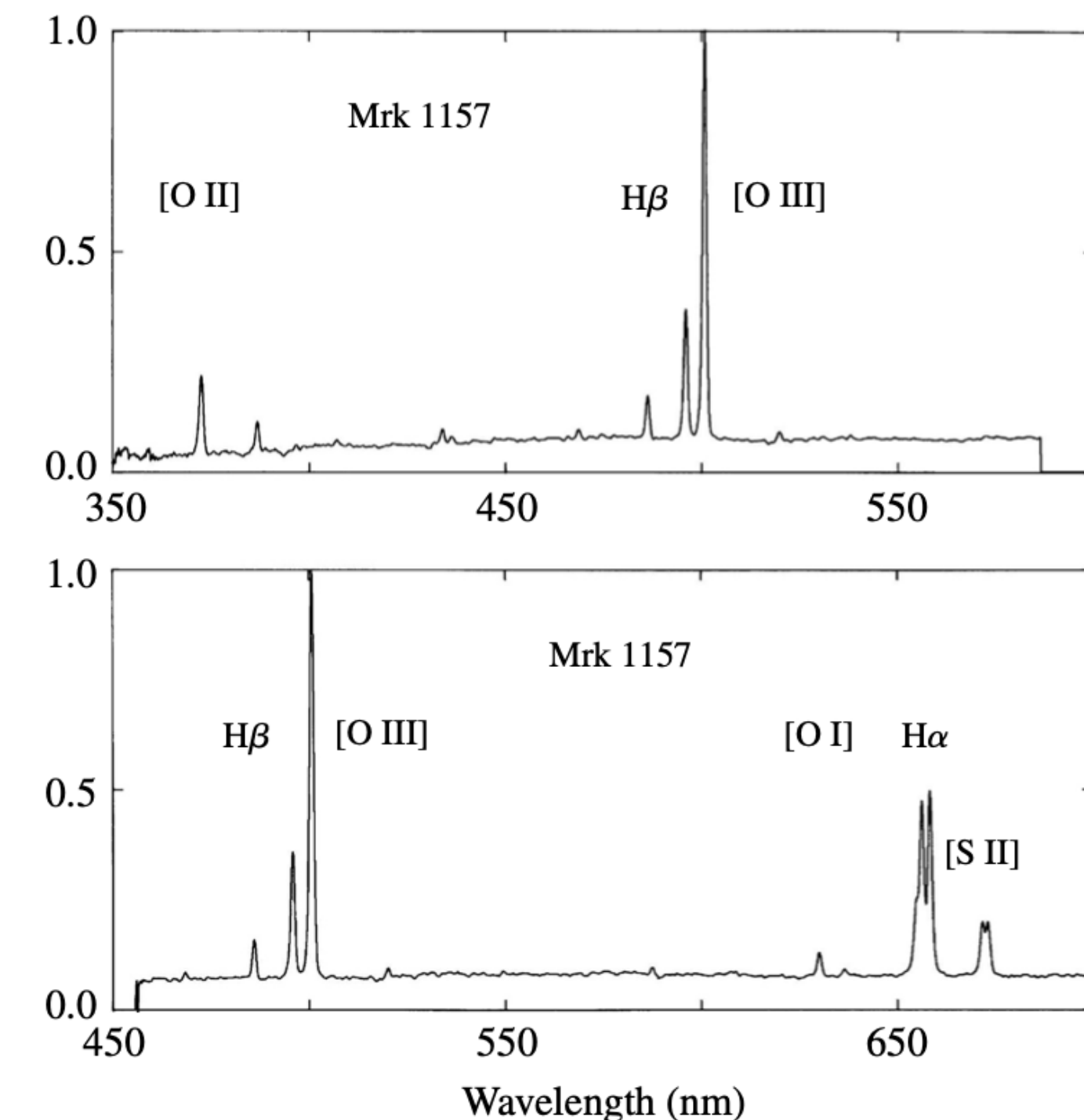


FIGURE 2 The visible spectrum of Mrk 1157, a Seyfert 2 galaxy. (Figure adapted from Osterbrock, *QJRAS*, 25, 1, 1984.)

Seyfert galaxies

Mrk 1157 - PanSTARS image

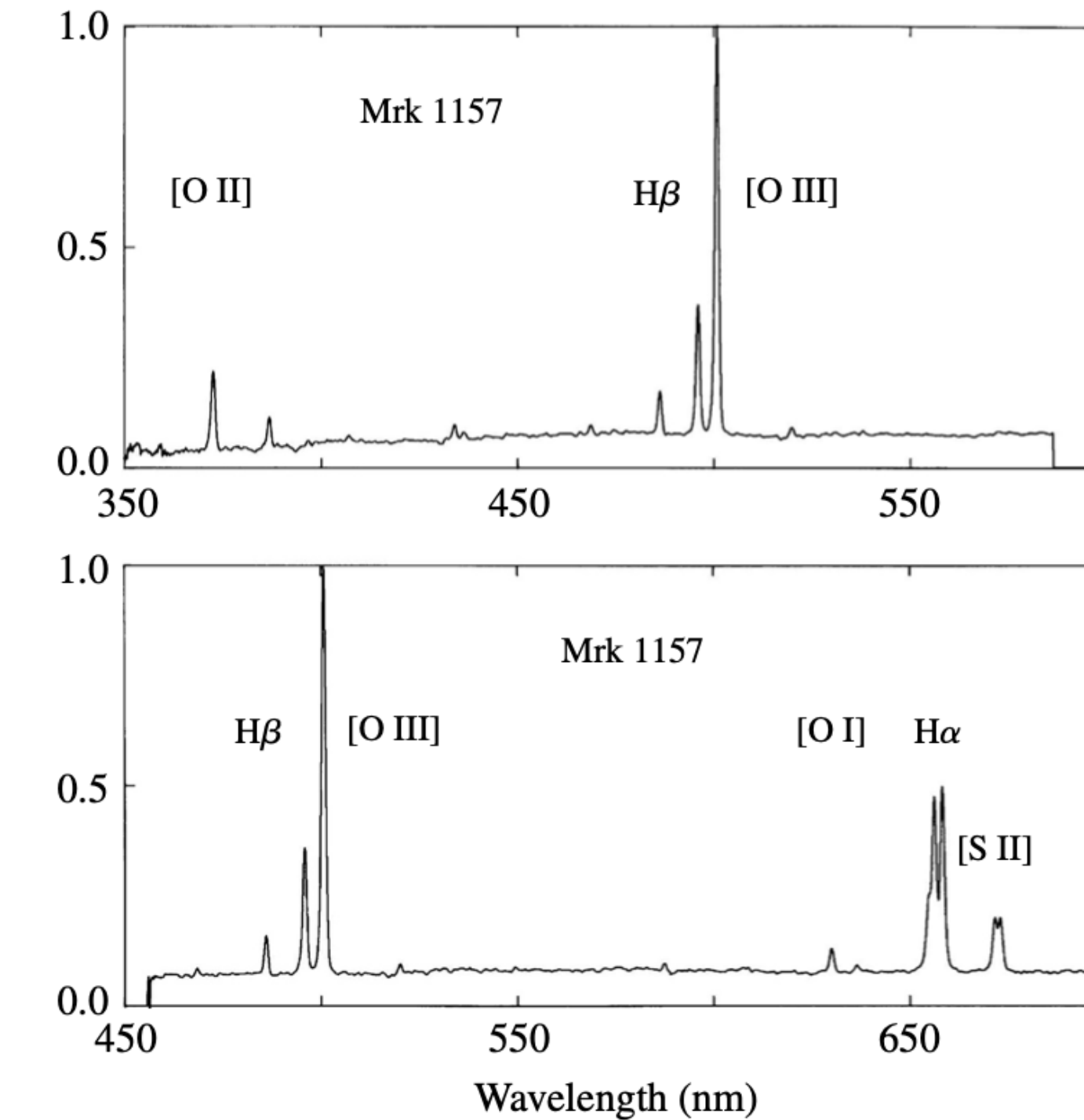
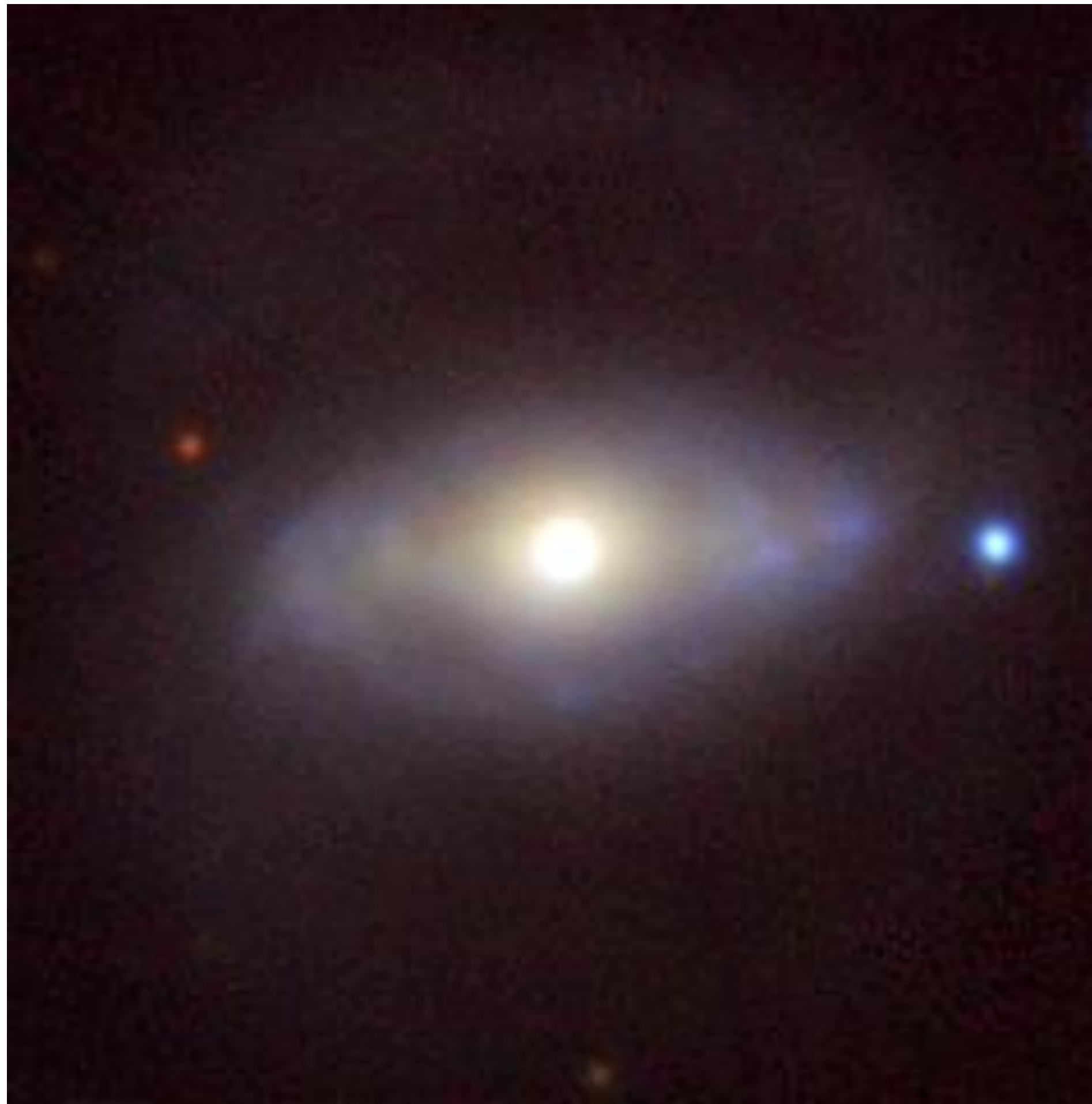


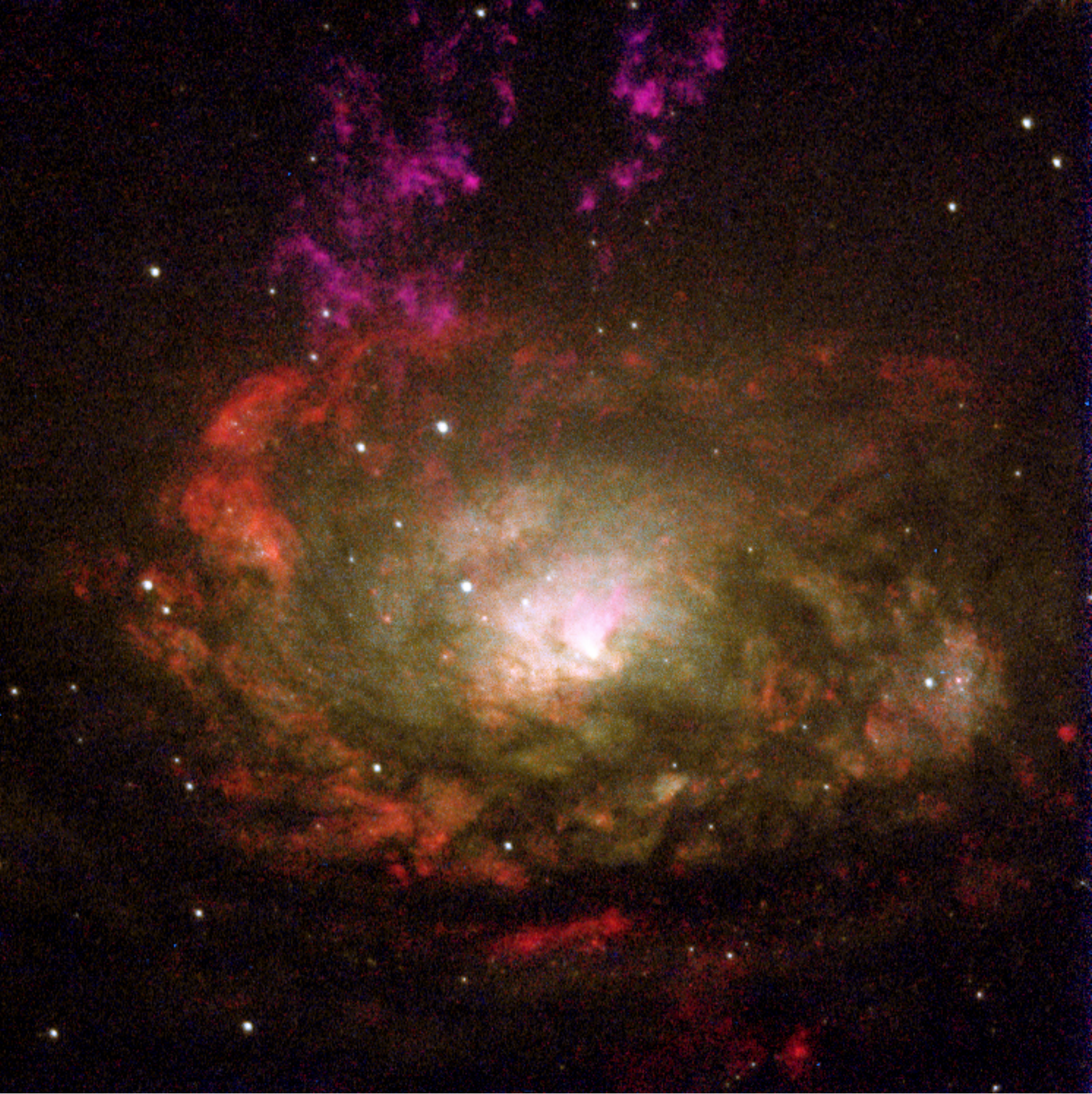
FIGURE 2 The visible spectrum of Mrk 1157, a Seyfert 2 galaxy. (Figure adapted from Osterbrock, *QJRAS*, 25, 1, 1984.)

Seyfert galaxies

The black hole-powered core of a nearby active galaxy appears in this colorful Hubble image. The galaxy lies 13 million light-years away in the southern constellation Circinus. This galaxy is designated a **type 2 Seyfert**.

AGN have the ability to remove gas from the centers of their galaxies by blowing it out into space at phenomenal speeds. Much of the gas in the disk of the Circinus spiral is concentrated in two specific rings — a larger one of diameter 1,300 light-years, and a previously unseen ring of diameter 260 light-years.

The smaller **inner ring is located on the inside of the green disk**. The **larger outer ring extends off the image** and is in the plane of the galaxy's disk. Both rings are home to large amounts of gas and dust as well as areas of major "**starburst**" activity, where new stars are rapidly forming on timescales of 40 - 150 million years, much shorter than the age of the entire galaxy.

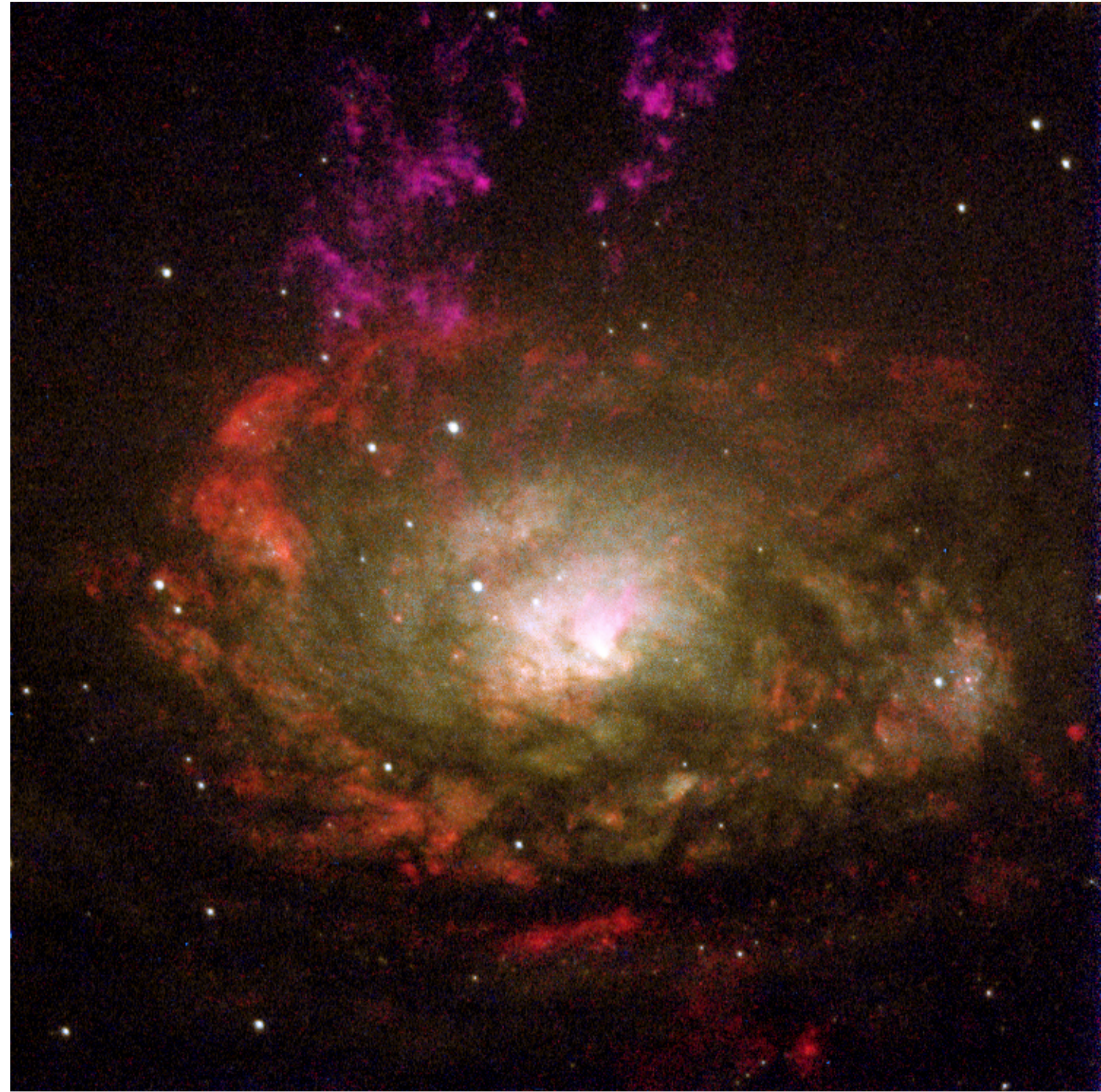


Seyfert galaxies

At the center of the starburst rings is the Seyfert nucleus, the supermassive black hole that is accreting. The black hole and its accretion disk are **expelling gas out of the galaxy's disk** and into its halo (the region above and below the disk). This gas is seen as **magenta-colored streamers** extending towards the top of the image.

In the center of the galaxy and within the inner starburst ring is a **V-shaped structure of gas**. The structure appears whitish-pink in this composite image. This region, which is the projection of a **three-dimensional cone** extending from the nucleus to the galaxy's halo, contains gas that has been heated by radiation emitted by the accreting black hole. A "counter-cone," believed to be present, is obscured from view by dust in the galaxy's disk.

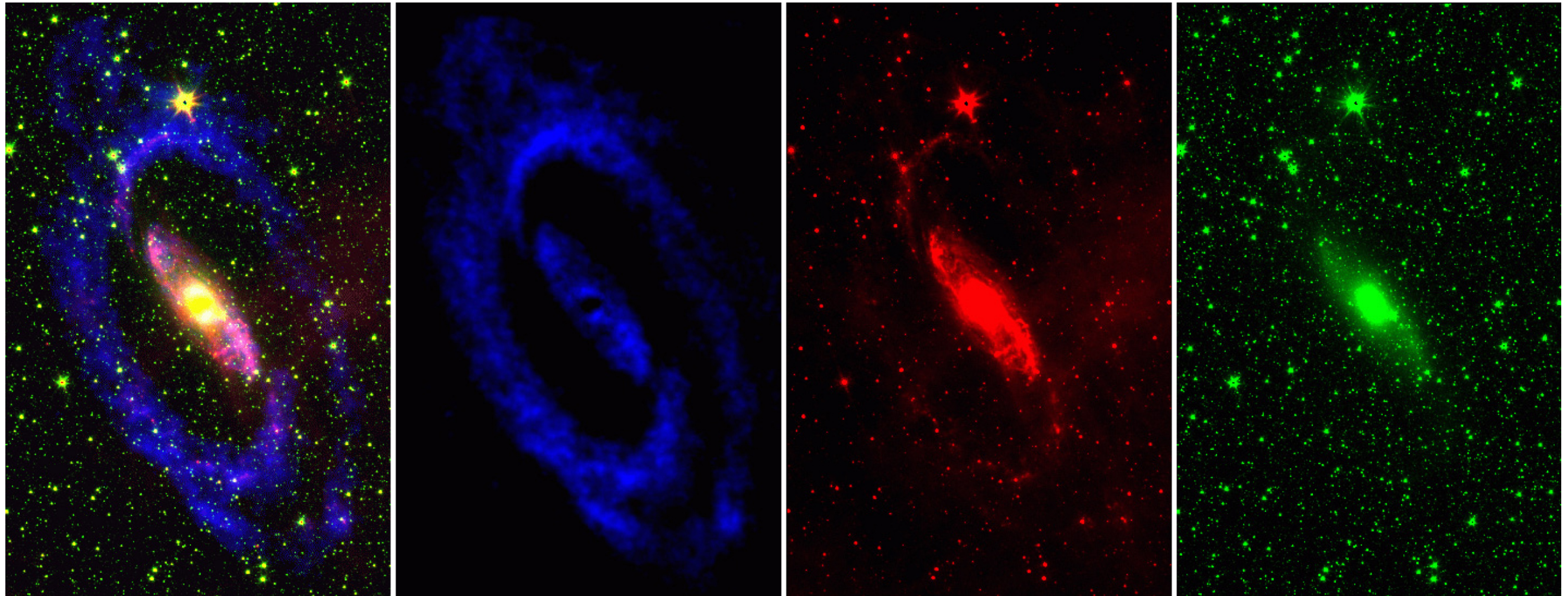
Ultraviolet radiation emerging from the central source excites nearby gas causing it to glow. **The excited gas is beamed into the oppositely directed cones** like two giant searchlights.



Seyfert galaxies

The **Circinus Galaxy** as seen at different wavelengths. The three single-color panels show the **ATCA HI gas distribution** at an angular resolution of 15 arcsec (only the inner disk is shown here), the **Spitzer 8 micron image** (PAH emission + stars) and the **Spitzer 3.6 micron image** (stars).

For et al 2012



Seyfert galaxies

Some spectra display **both broad and narrow permitted lines**, and so they are classified as an **intermediate type** such as Seyfert 1.5. However, it is important to emphasize that this is a spectral classification. The **spectra of a few Seyfert galaxies have changed nearly from type 1.5 to type 2 in a matter of years**, although the broad H α emission line has rarely if ever completely disappeared.

The galaxies known to emit the **most X-ray energy are Seyferts of types 1 and 1.5**. The X-ray emission is quite **variable**, and can change appreciably on **timescales ranging from days to hours**.

In contrast, **X-rays are less frequently measured for Seyfert 2** galaxies. An analysis of the hard X-rays that are observed for Seyfert 2s indicates that the “missing” X-rays have been **absorbed by intervening material with huge hydrogen column densities** of between 10^{26} and 10^{28} m^{-2} .

Seyferts make up only a few tenths of a percent of all field galaxies.

It is interesting that at least **90%** of the Seyferts close enough to be resolved by telescopes are **spiral galaxies**, typically of types Sb or SBb.

Seyfert galaxies

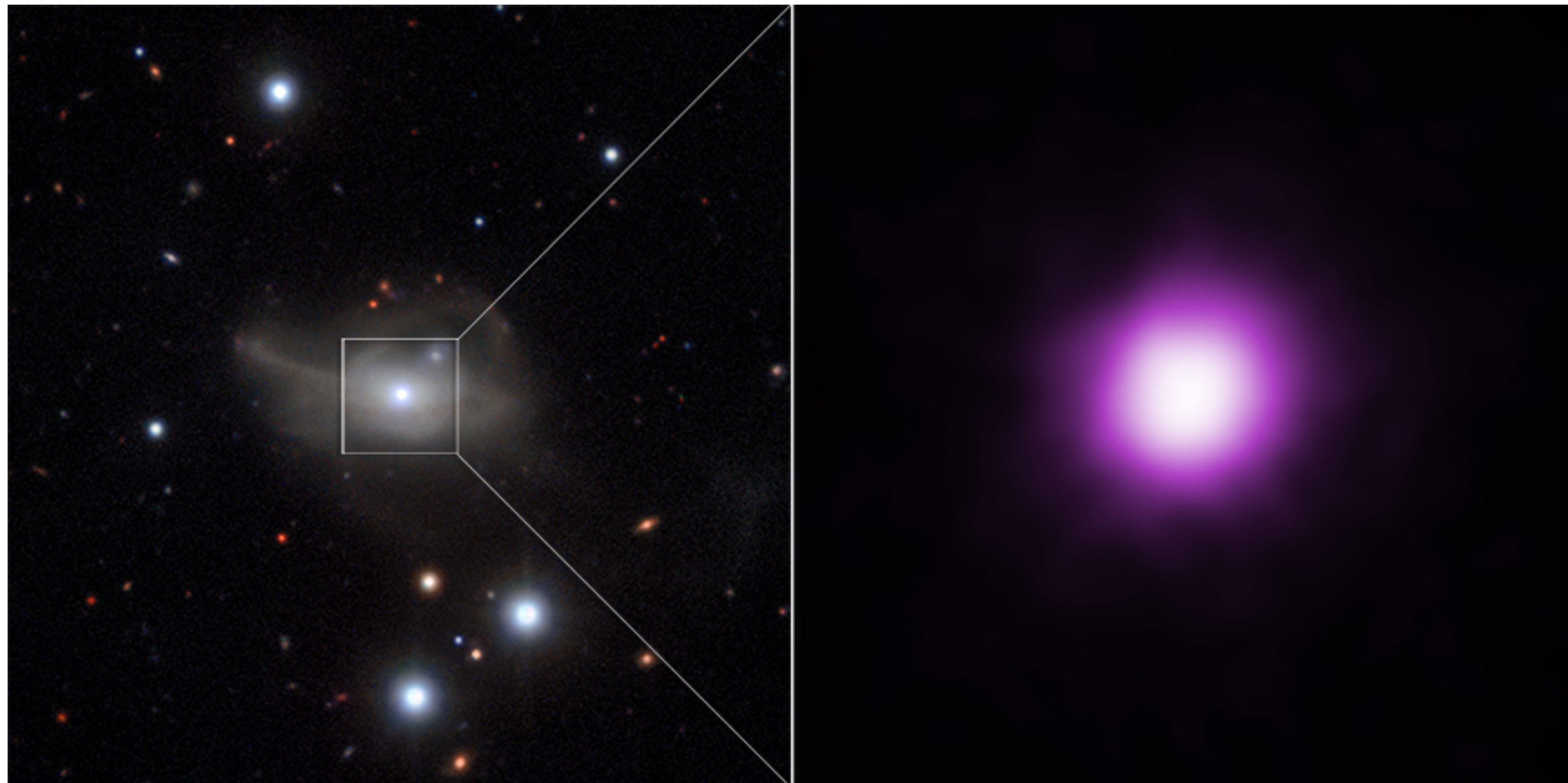
They are **frequently accompanied by other galaxies** with which they may be gravitationally interacting.
Seyfert galaxy **NGC 4151** (type Sab) with a galactic disk around its bright nucleus + some outer spiral arms.



Seyfert galaxies

The galaxy Markarian 1018 stands out by changing type twice, from a faint to a bright AGN in the 1980s and then changing back to a faint AGN within the last five years. A handful of AGN have been observed to make this full-cycle change. During the second change in type the Markarian 1018 AGN became eight times fainter in [X-rays](#) between 2010 and 2016.

The AGN had faded because the black hole was being starved of infalling material. This starvation also explains the fading of the AGN in X-rays.



The spectra

Seyferts belong to the general class of galaxies with **active galactic nuclei**, or AGN for short. Other members of this class, such as radio galaxies, quasars, and blazars.

Figure 4 is a rough schematic of the continuum observed for many types of AGNs (note that the logarithm of the product νF_ν is plotted on the figure's vertical axis). The most notable feature of this **spectral energy distribution (SED)** is its persistence over some **10 orders of magnitude in frequency**. This wide spectrum is markedly **different from the thermal (blackbody) spectrum** of a star or the combined spectra of a galaxy of stars.

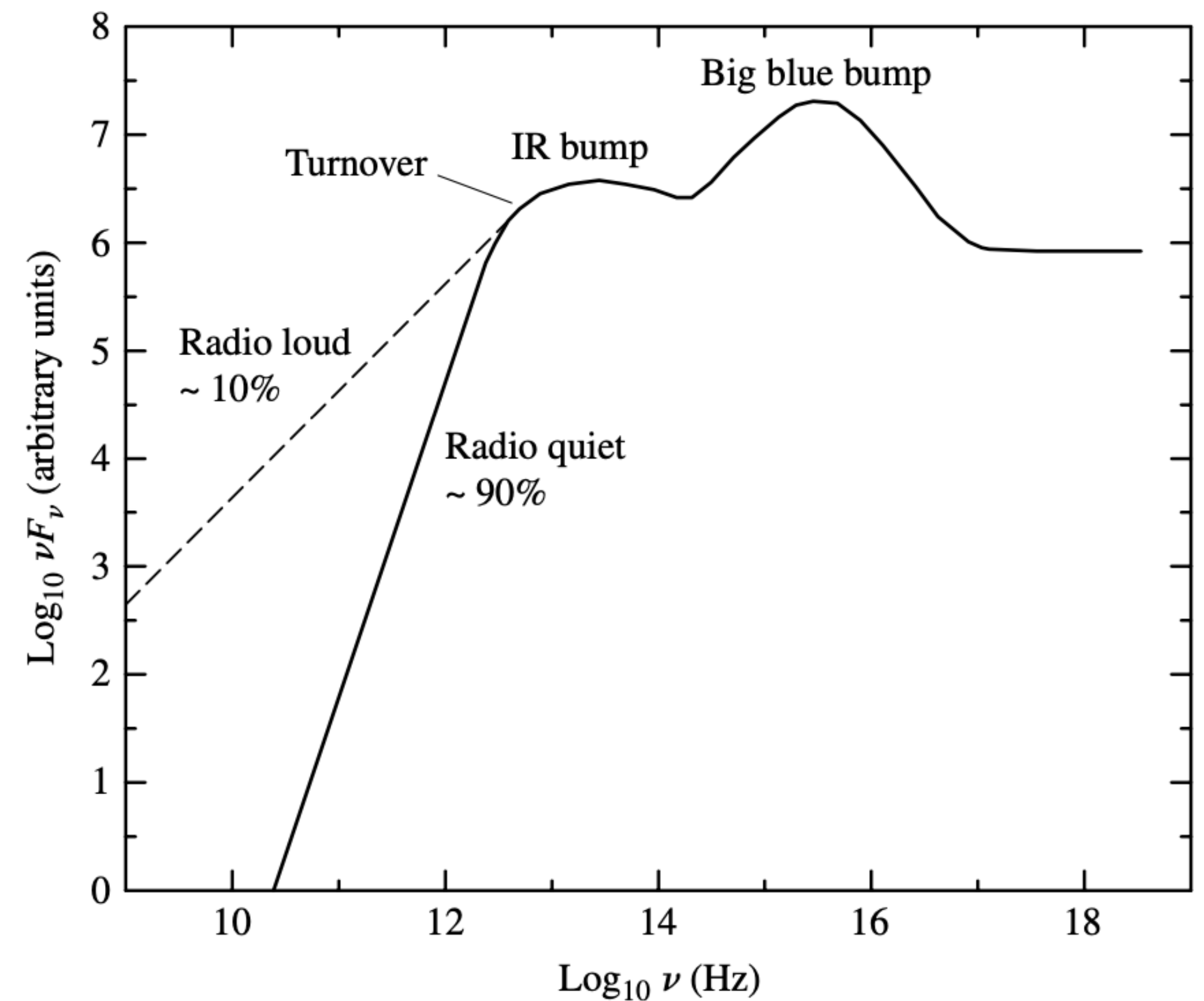


FIGURE 4 A sketch of the continuum observed for many types of AGNs.

The spectra

When AGNs were first studied, it was thought that their spectra were quite flat. Accordingly, a power law of the form

$$F_\nu \propto \nu^{-\alpha}$$

was used to describe the monochromatic energy flux, F_ν . The **spectral index**, α , was believed to have a value of $\alpha \approx 1$.

The power received within any frequency interval between ν_1 and ν_2 is

$$L_{\text{interval}} \propto \int_{\nu_1}^{\nu_2} F_\nu d\nu = \int_{\nu_1}^{\nu_2} \nu F_\nu \frac{d\nu}{\nu} = \ln 10 \int_{\nu_1}^{\nu_2} \nu F_\nu d \log_{10} \nu,$$

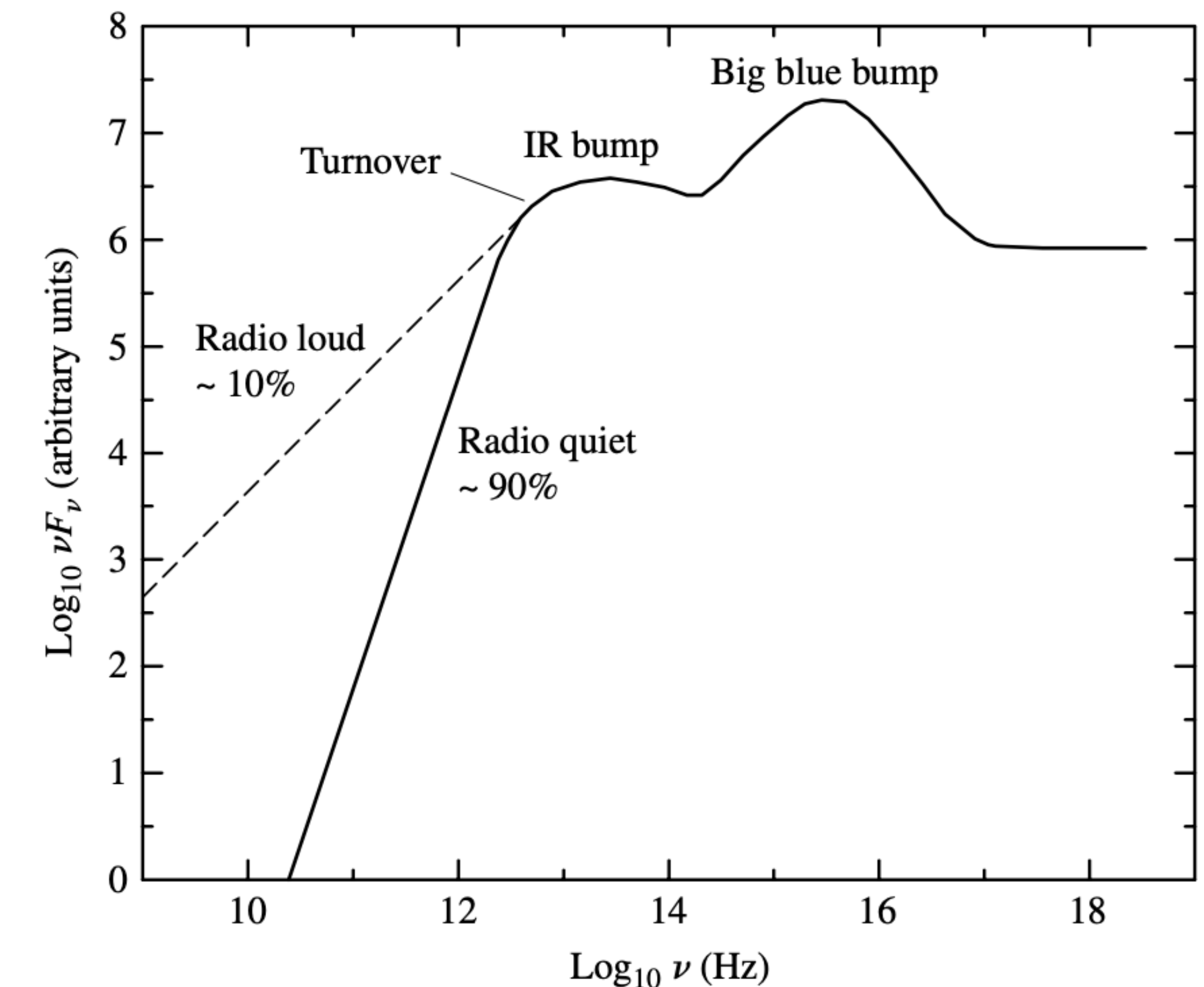


FIGURE 4 A sketch of the continuum observed for many types of AGNs.

The spectra

so that **equal areas under a graph of νF_ν vs. $\log_{10} \nu$** correspond to **equal amounts of energy**; hence the reason for plotting $\log_{10} \nu F_\nu$ on the ordinate in Fig. 4.

A value of $\alpha \approx 1$ reflects the **horizontal trend** seen to the right of the turnover in Fig. 4.

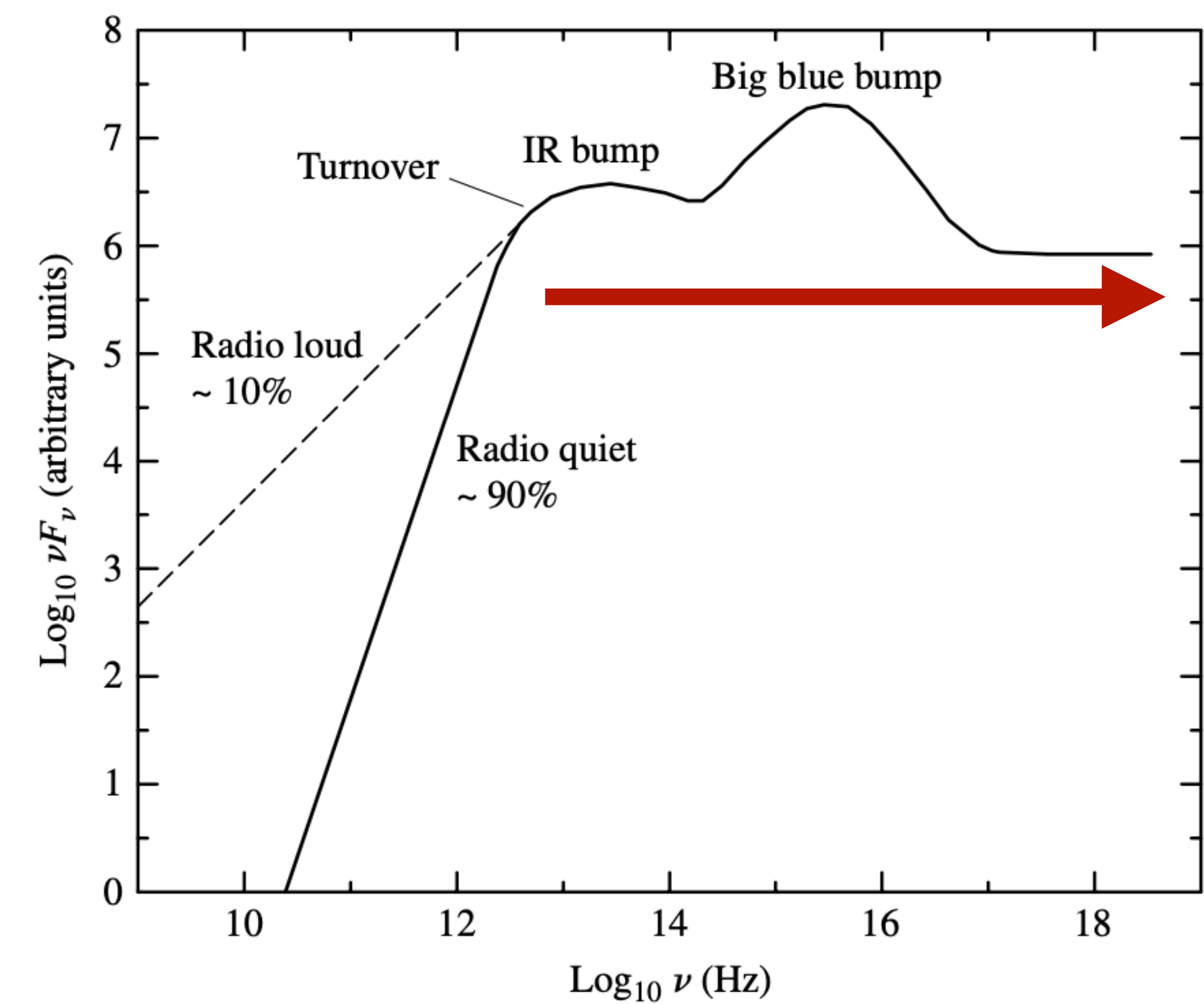


FIGURE 4 A sketch of the continuum observed for many types of AGNs.

The spectra

The continuous spectra of AGNs are now known to be more complicated, involving a mix of thermal and nonthermal emission. However, this is still used to *parameterize* the continuum.

The **spectral index typically has a value between 0.5 and 2 that usually increases with increasing frequency**, so the curve of $\log_{10} \nu F_\nu$ vs. $\log_{10} \nu$ in Fig. 4 is generally concave downward.

In fact, the value of α is **constant over only a limited range of frequencies**, such as in the infrared and visible regions of the spectrum. The shape and polarization of the visible-UV spectrum indicates that it can sometimes be decomposed into contributions from thermal sources (**blackbody spectrum, low polarization**) and nonthermal sources (**power-law spectrum, significant polarization**).

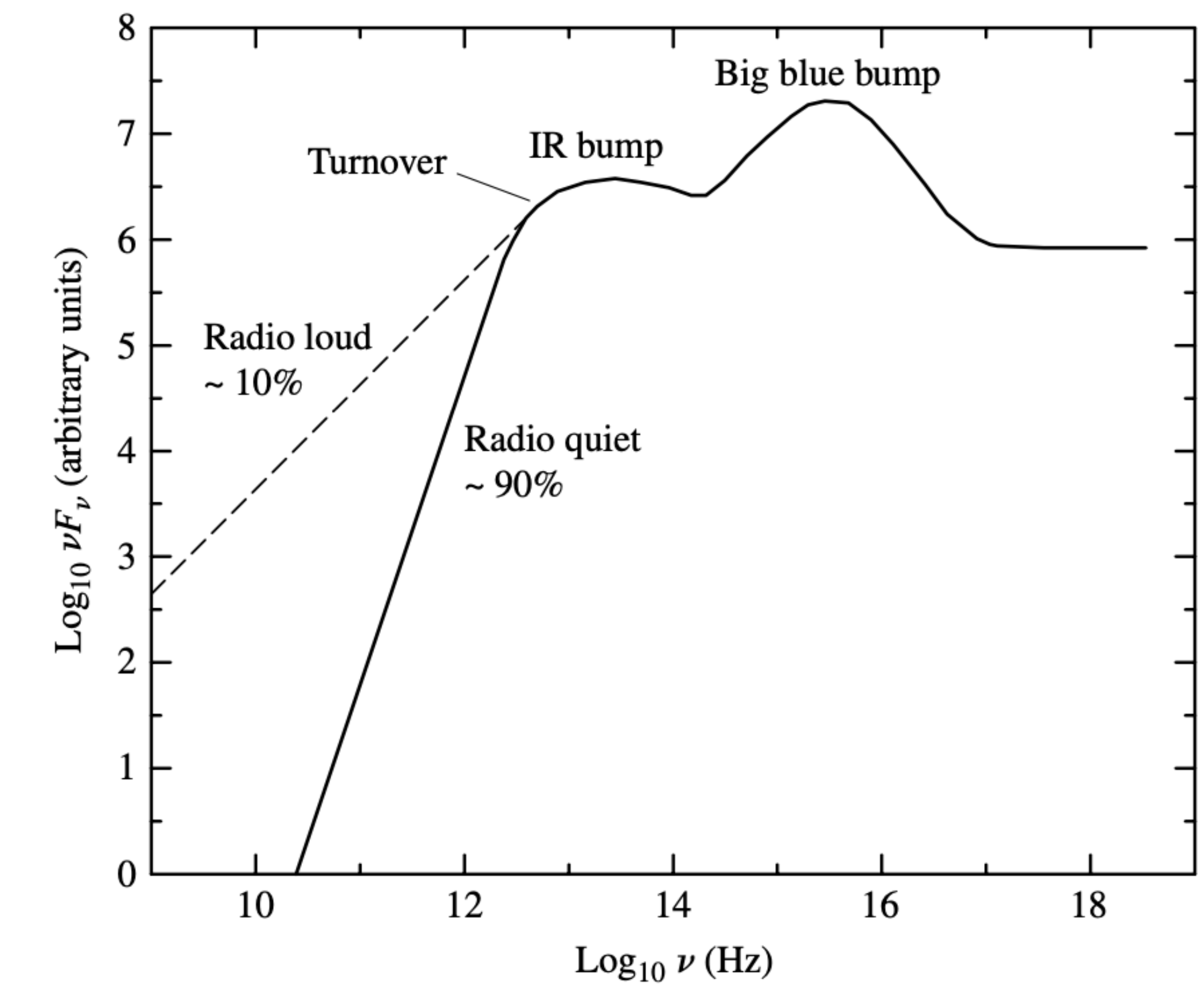


FIGURE 4

A sketch of the continuum observed for many types of AGNs.

The spectra

The **thermal component** appears as the **big blue bump** in Fig. 4, which can contain an appreciable amount of the bolometric luminosity of the source.

It is generally believed that the emission from the big blue bump is **due to an optically thick accretion disk**, although some researchers have suggested that free-free emission may be responsible.

Also evident is a thermal **infrared bump** to the left of the big blue bump; it is probably due to emission from warm ($T < 2000$ K) dust grains.

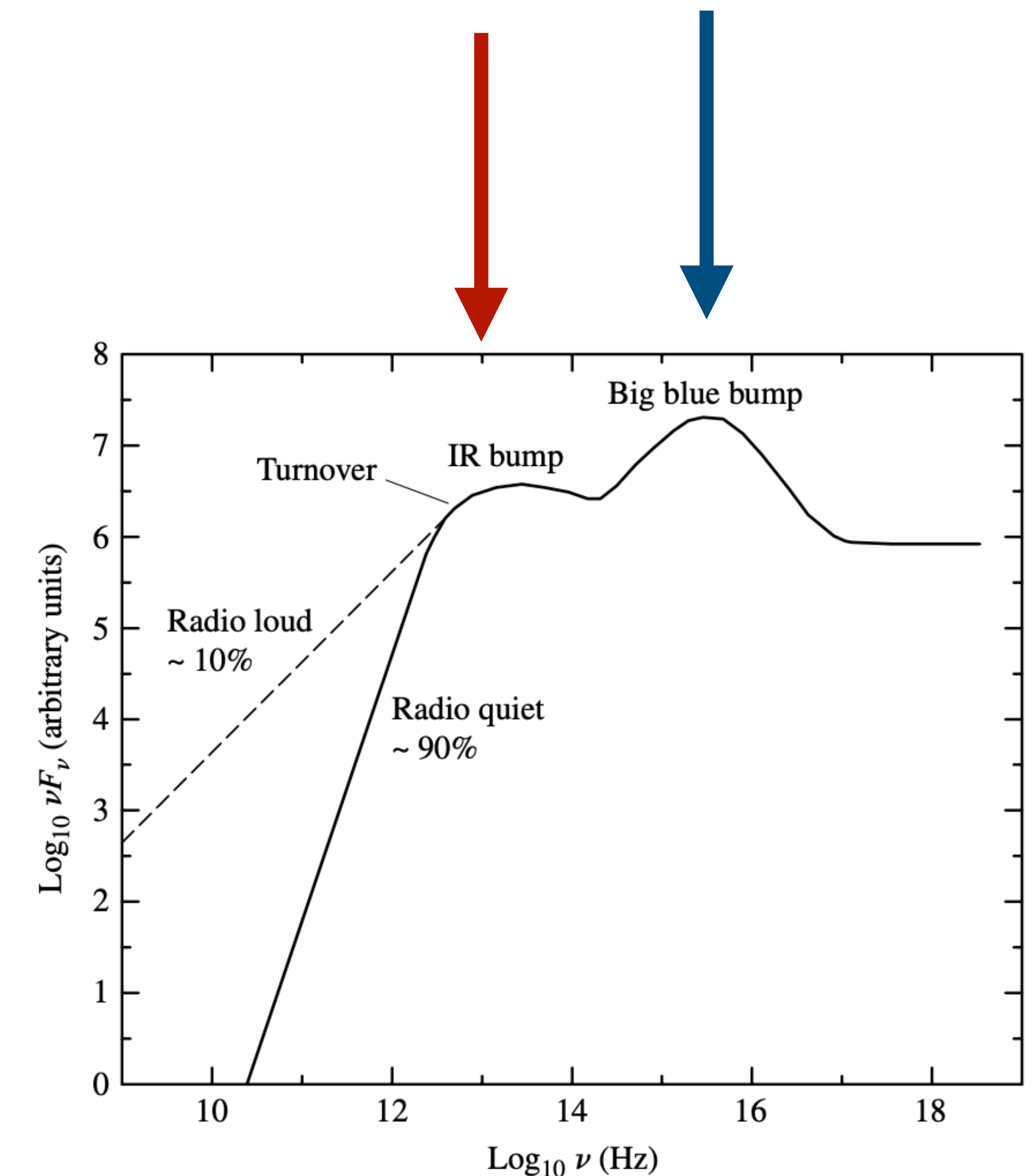


FIGURE 4 A sketch of the continuum observed for many types of AGNs.

The spectra

A pure power-law spectrum (with constant α) is the signature of synchrotron radiation, which is frequently encountered in astronomical situations involving relativistic electrons and magnetic fields.

As shown in Fig. 5, a synchrotron spectrum is produced by the combined radiation emitted by individual electrons as they spiral around magnetic field lines. If the distribution of the individual electron energies obeys a power law, then the resulting synchrotron spectrum is described by Eq. (1).

However, the synchrotron spectrum does not continue to rise without limit as the frequency decreases. **At a transition frequency, the spectrum turns over** and varies as $\nu^{5/2}$ (spectral index $\alpha = -2.5$). This occurs because **the plasma of spiraling electrons becomes opaque to its own synchrotron radiation**, an effect known as **synchrotron self-absorption**.

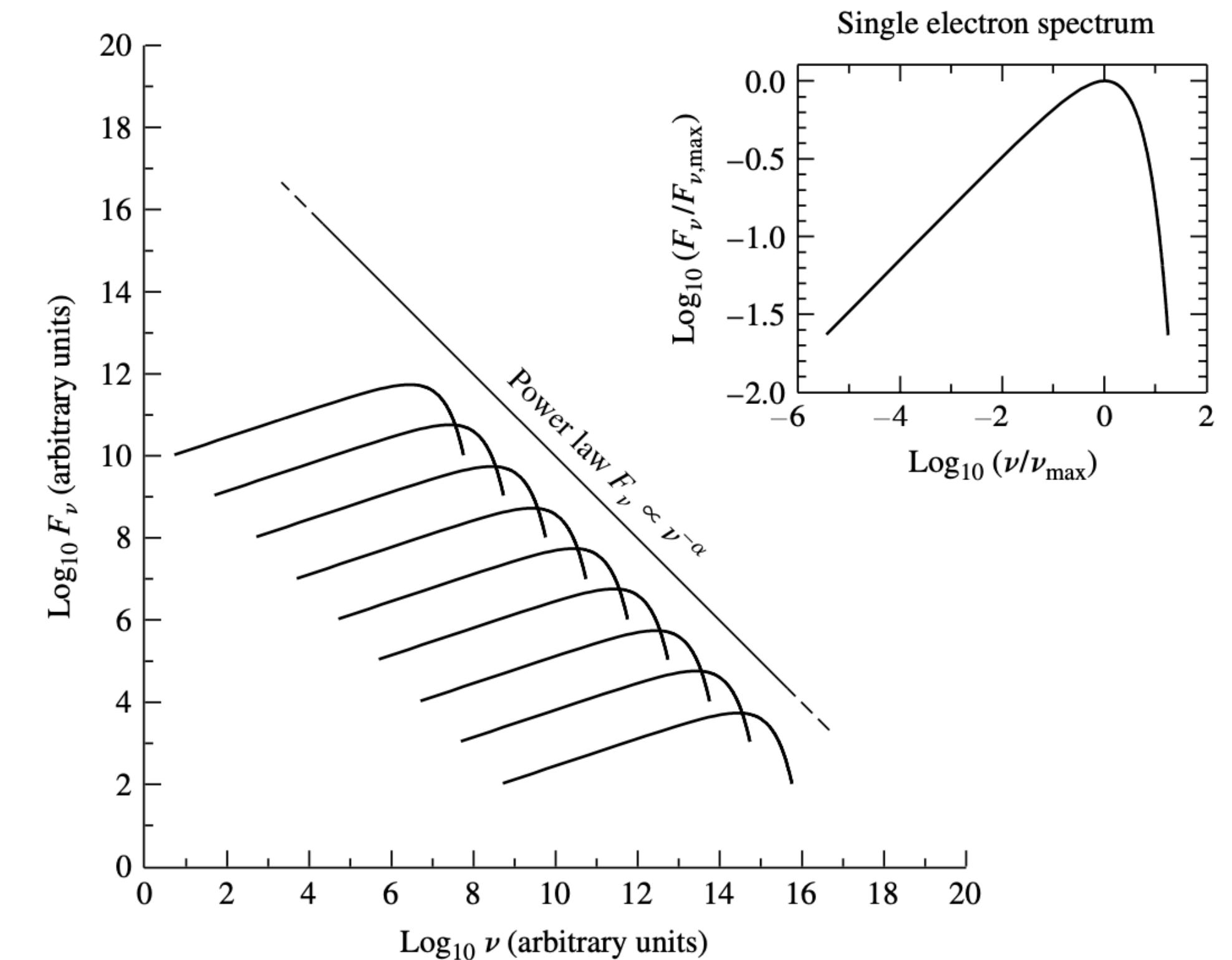


FIGURE 5 The power-law spectrum of synchrotron radiation, shown as the sum of the radiation produced by individual electrons as they spiral around magnetic field lines. The spectrum of a single electron is at the upper right. The turnover at low frequencies is not shown.

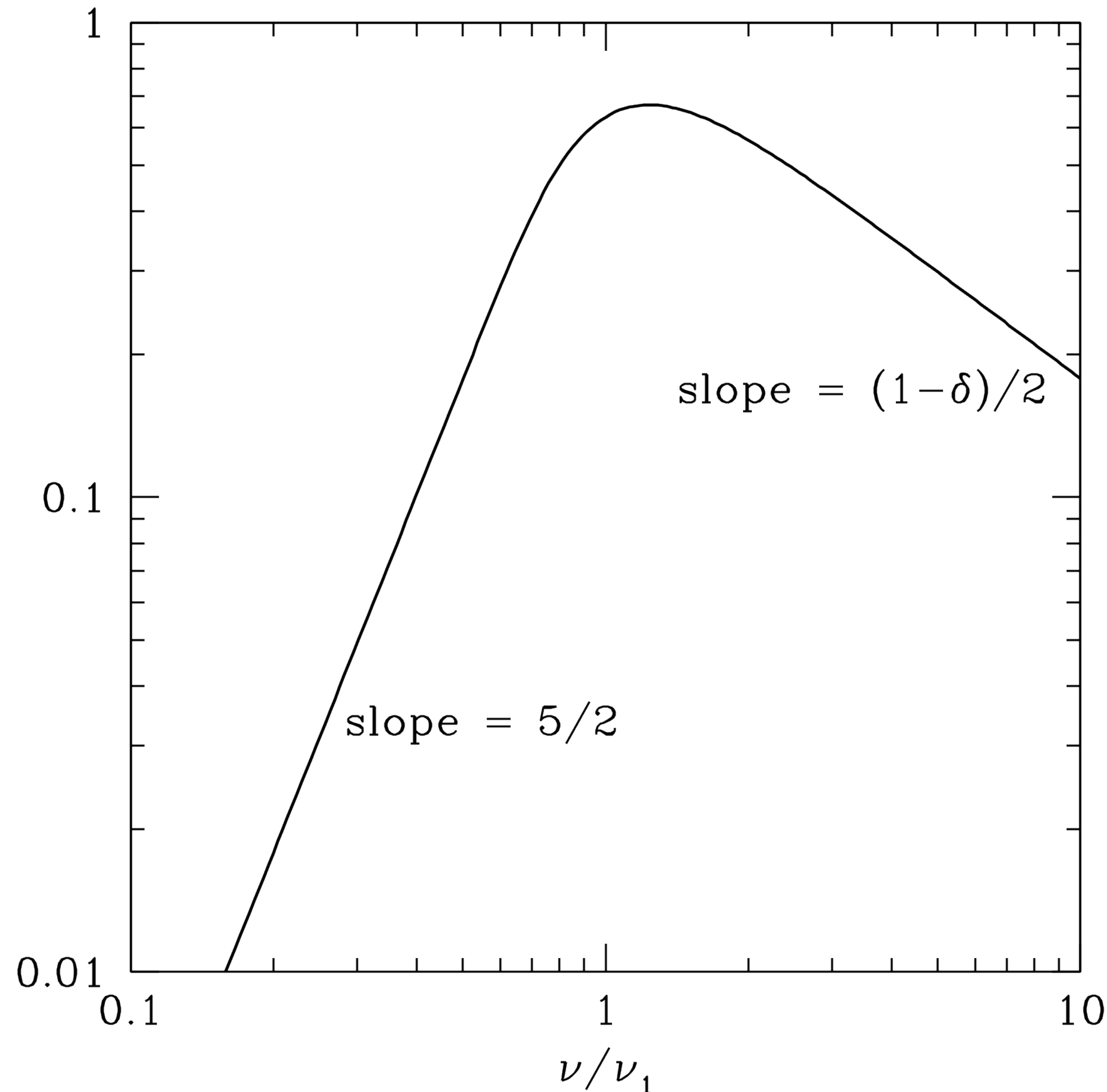
The spectra

A pure power-law spectrum (with constant α) is the signature of synchrotron radiation, which is frequently encountered in astronomical situations involving relativistic electrons and magnetic fields.

As shown in Fig. 5, a synchrotron spectrum is produced by the combined radiation emitted by individual electrons as they spiral around magnetic field lines. If the distribution of the individual electron energies obeys a power law, then the resulting synchrotron spectrum is described by Eq. (1).

However, the synchrotron spectrum does not continue to rise without limit as the frequency decreases. **At a transition frequency, the spectrum turns over** and varies as $\nu^{5/2}$ (spectral index $\alpha = -2.5$). This occurs because **the plasma of spiraling electrons becomes opaque to its own synchrotron radiation**, an effect known as **synchrotron self-absorption**.

homogeneous cylindrical synchrotron source in terms of the frequency at ν_1 at which $\tau = 1$. Real astrophysical sources are inhomogeneous, so their low-frequency spectral slopes are smaller than 5/2 and their spectral peaks are not so sharp.



The spectra

In some SEDs (Spectral energy distribution), the “turnover” evident in the schematic continuum spectrum in Fig. 4 may be due to synchrotron self-absorption.

However, the **thermal contributions to the continuum spectrum evident in the infrared bump suggest** that in other cases, the turnover may be due to the long-wavelength Rayleigh–Jeans portion of the blackbody spectrum produced by the warm dust grains.

It is possible that the steeper, low-frequency spectra of radio-quiet AGNs are due to the thermal spectrum of dust grains, while the shallower, low-frequency spectra of radio-loud AGNs **may be due to a combination of thermal and nonthermal emission.**

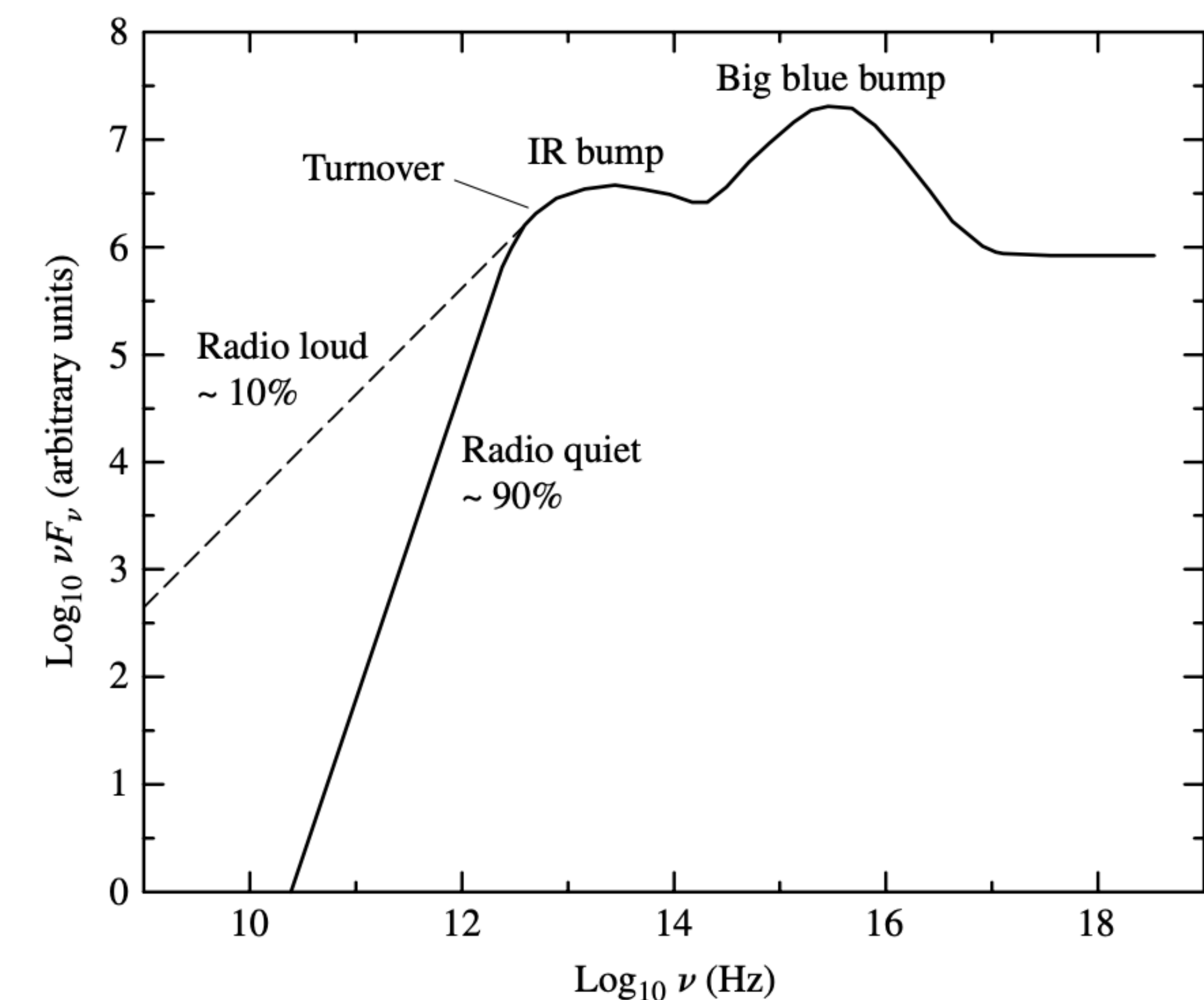
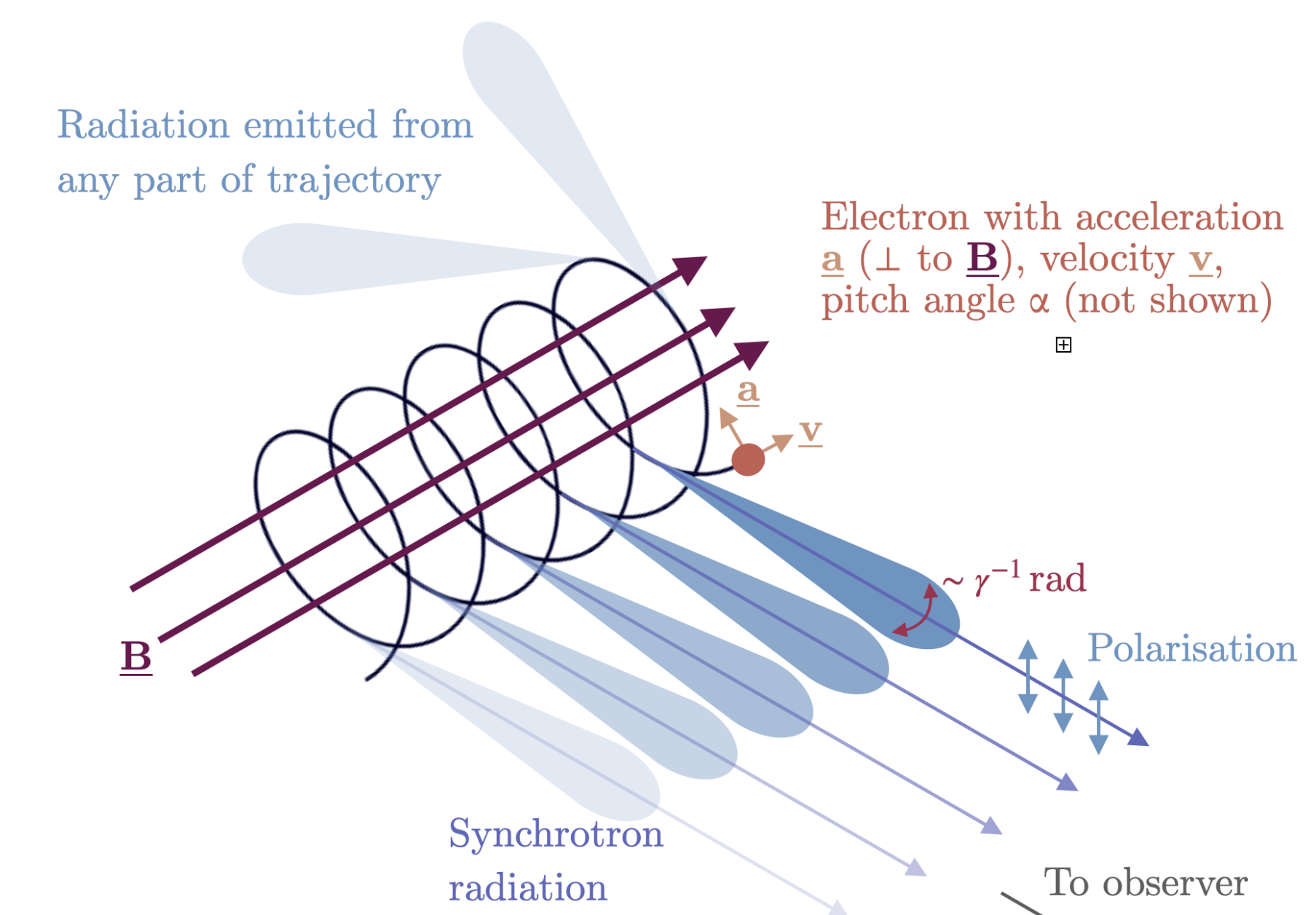


FIGURE 4 A sketch of the continuum observed for many types of AGNs.

Synchrotron radiation

- **Synchrotron radiation is the electromagnetic radiation emitted when relativistic charged particles are subject to an acceleration perpendicular to their velocity.** It is produced naturally by fast electrons moving through magnetic fields. The radiation produced in this way has a characteristic polarization and the frequencies generated can range over a large portion of the electromagnetic spectrum.
- Synchrotron radiation is similar to bremsstrahlung radiation, which is emitted by a charged particle when the acceleration is parallel to the direction of motion.
- The **general term for radiation emitted by particles in a magnetic field is gyromagnetic radiation**, for which synchrotron radiation is the ultra-relativistic special case. Radiation emitted by charged particles moving non-relativistically in a magnetic field is called cyclotron emission. For particles in the mildly relativistic range ($\approx 85\%$ of the speed of light), the emission is termed gyro-synchrotron radiation.



Emma Alexander

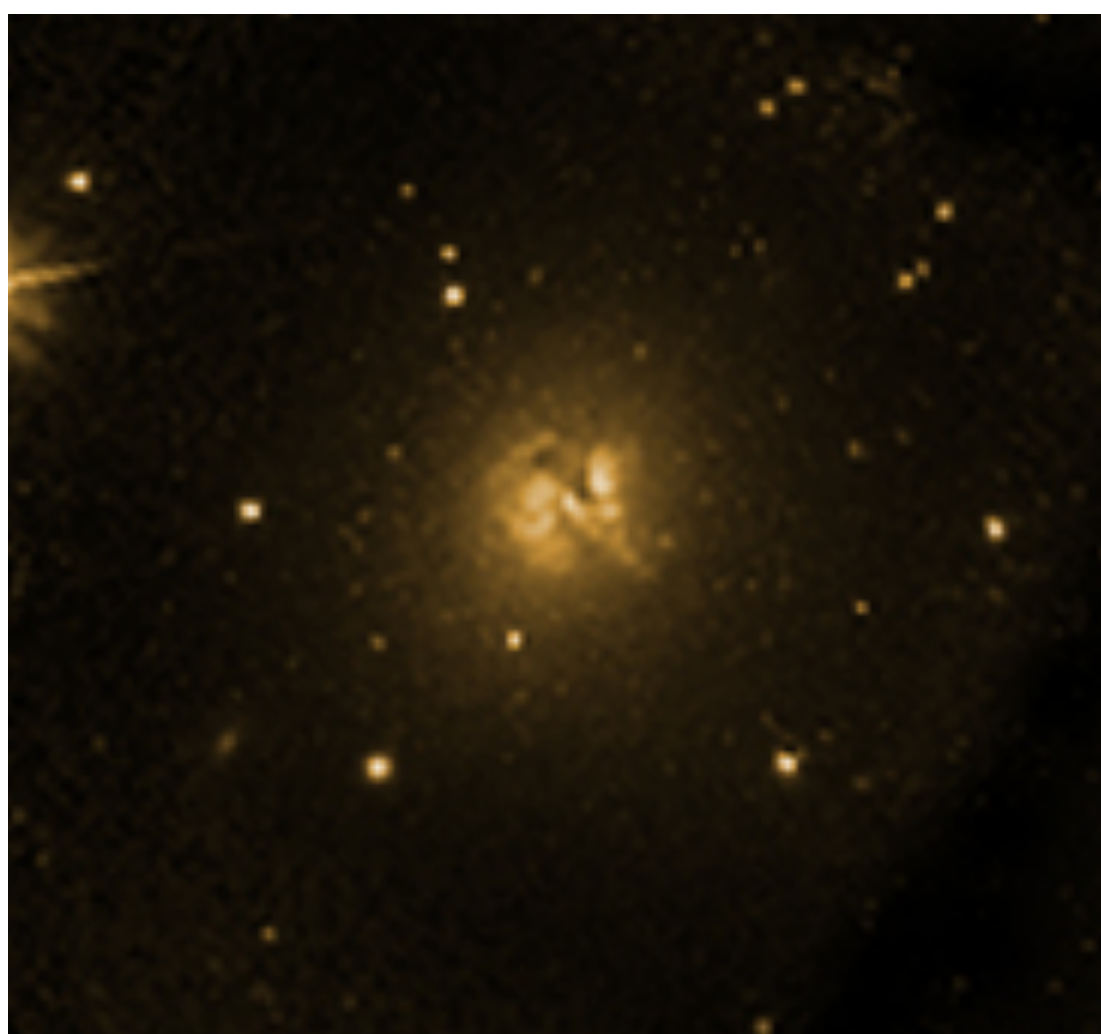
Radio Galaxies

The first discrete source of strong radio waves (other than the Sun) was discovered in the constellation Cygnus and was named Cygnus A.

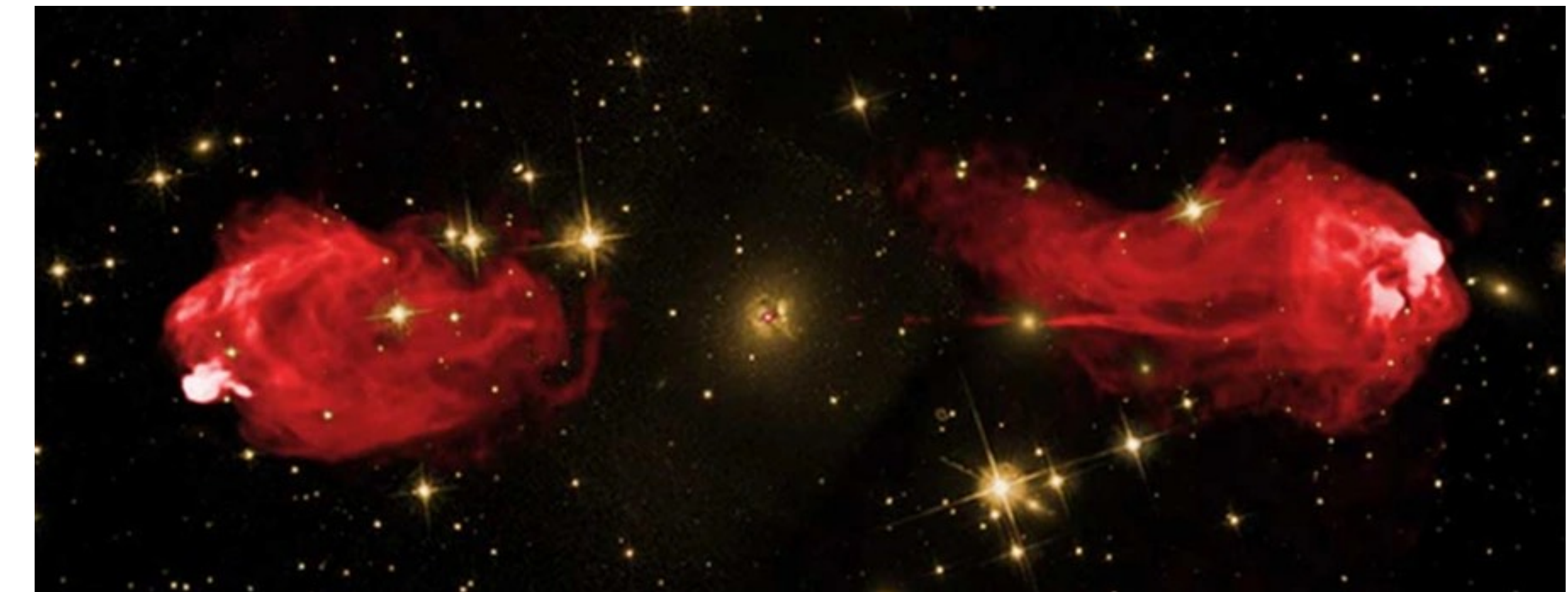
Using the accurate position provided by radio astronomy the optical counterpart of Cyg A. It is a **peculiar-looking cD galaxy** whose center is apparently encircled by a **ring of dust**.

Cyg A's spectrum shows a redshift of $z = \Delta\lambda/\lambda_{rest} = 0.057$, corresponding to a recessional velocity of 16,600 km s⁻¹. From Hubble's law, the distance to Cyg A is about 170h⁻¹ Mpc (implying a distance of 240 Mpc if h = [h]_{WMAP}).

Considering that Cyg A is the brightest radio source beyond the Milky Way, this **distance is surprisingly large**.



Cyg A - radio galaxy (AGN)

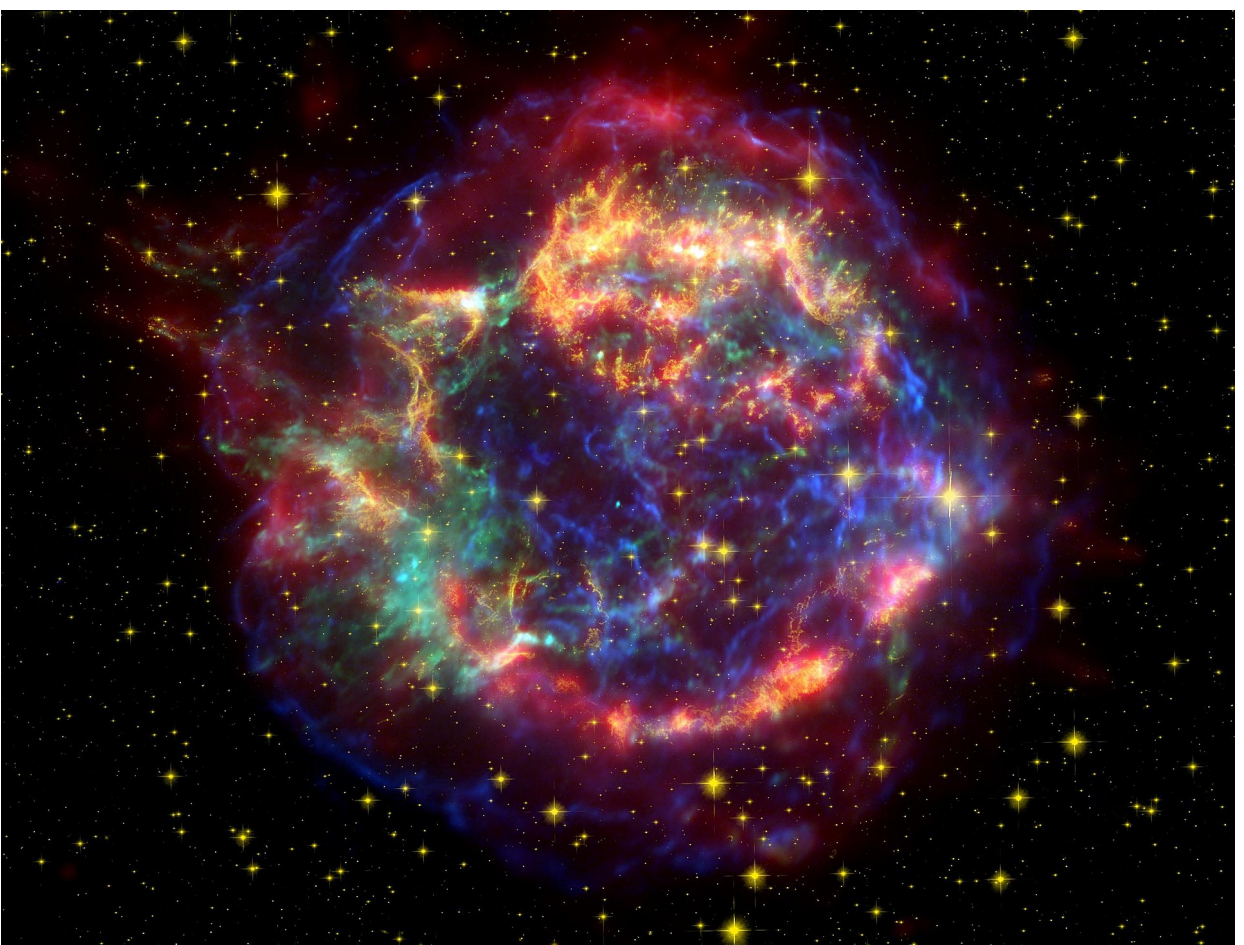


Radio Galaxies

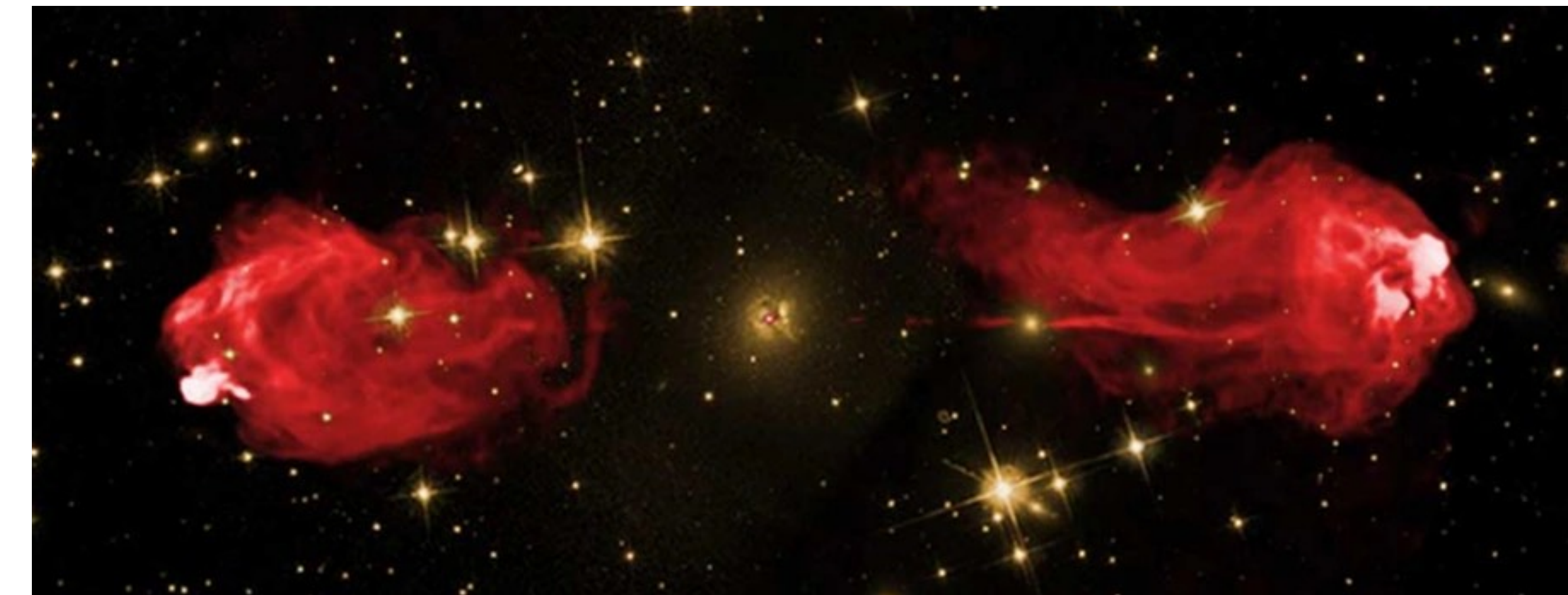
In fact, the only discrete radio sources brighter than Cyg A are the Sun and Cassiopeia A, the nearby (3 kpc) remnant of a Type II supernova. **To be detected so far away, Cyg A must pour out enormous amounts of radio energy.**

Cyg A is one example of a class of galaxies, called **radio galaxies**, that are **extremely bright at radio wavelengths**.

Cas A - Supernova remnant



Cyg A - radio galaxy (AGN)



Radio Galaxies



Example 1.1. The radio energy emitted by Cygnus A can be estimated by using its distance of $d = 170 h^{-1}$ Mpc together with the observed value of the monochromatic flux at a radio frequency of 1400 MHz,

$$F_{1400} = 1.255 \times 10^{-23} \text{ W m}^{-2} \text{ Hz}^{-1} = 1255 \text{ Jy}.$$

The radio spectrum follows the power law of Eq. (1) with $\alpha \approx 0.8$, so $F_\nu \propto \nu^{-0.8}$. That is, we can write

$$F_\nu = F_{1400} \left(\frac{\nu}{1400 \text{ MHz}} \right)^{-0.8}.$$

The radio luminosity can be found by integrating the monochromatic flux over the range of radio frequencies. The upper frequency limit is taken to be $\nu_2 = 3 \times 10^9$ Hz, corresponding to a radio wavelength of 0.1 m. The power-law behavior of the radio spectrum does not continue to $\nu = 0$. Instead, the flux received from Cygnus A declines when the frequency falls below about $\nu_1 = 10^7$ Hz.

Radio Galaxies



With these limits, the radio luminosity is approximately

$$L_{\text{radio}} = 4\pi d^2 \int_{\nu_1}^{\nu_2} F_{\nu} d\nu = 4\pi d^2 F_{1400} \int_{\nu_1}^{\nu_2} \left(\frac{\nu}{1400 \text{ MHz}} \right)^{-0.8} d\nu = 2.4 \times 10^{37} h^{-2} \text{ W.}$$

Using the WMAP value of $[h]_{\text{WMAP}} = 0.71$, the radio luminosity of Cygnus A is estimated to be $L_{\text{radio}} = 4.8 \times 10^{37}$ W. This is **several million times more radio energy than is produced by a normal galaxy** such as M31 and is roughly three times the energy produced at *all* wavelengths by the Milky Way.



M31 - Andromeda galaxy

Radio Galaxies



Like Seyfert galaxies, radio galaxies may also be divided into two classes:

- **broad-line radio galaxies** (BLRGs, corresponding to Seyfert 1s) and
- **narrow-line radio galaxies** (NLRGs, corresponding to Seyfert 2s).

BLRGs have bright, starlike nuclei surrounded by very faint, hazy envelopes.

NLRGs, on the other hand, are giant or supergiant elliptical galaxies (types cD, D, and E); Cyg A is a NLRG.

Despite their similarities, there are obvious differences between Seyferts and radio galaxies. Although **Seyfert nuclei emit some radio energy**, they are **relatively quiet at radio wavelengths** compared with radio galaxies. Furthermore, while nearly all **Seyferts are spiral galaxies**, **none of the strong radio galaxies are spirals**.

Radio lobes and jets



A radio galaxy may display extended **radio lobes**, or it may radiate its energy both from a compact **core** in its nucleus and from a **halo** that is about the size of the visible galaxy or larger.

Cyg A -> The optical galaxy is flanked by two huge radio lobes that are the sources of the tremendous radio luminosity estimated in Example 1.1. Each of the lobes has a diameter of about 17h^{-1} kpc.

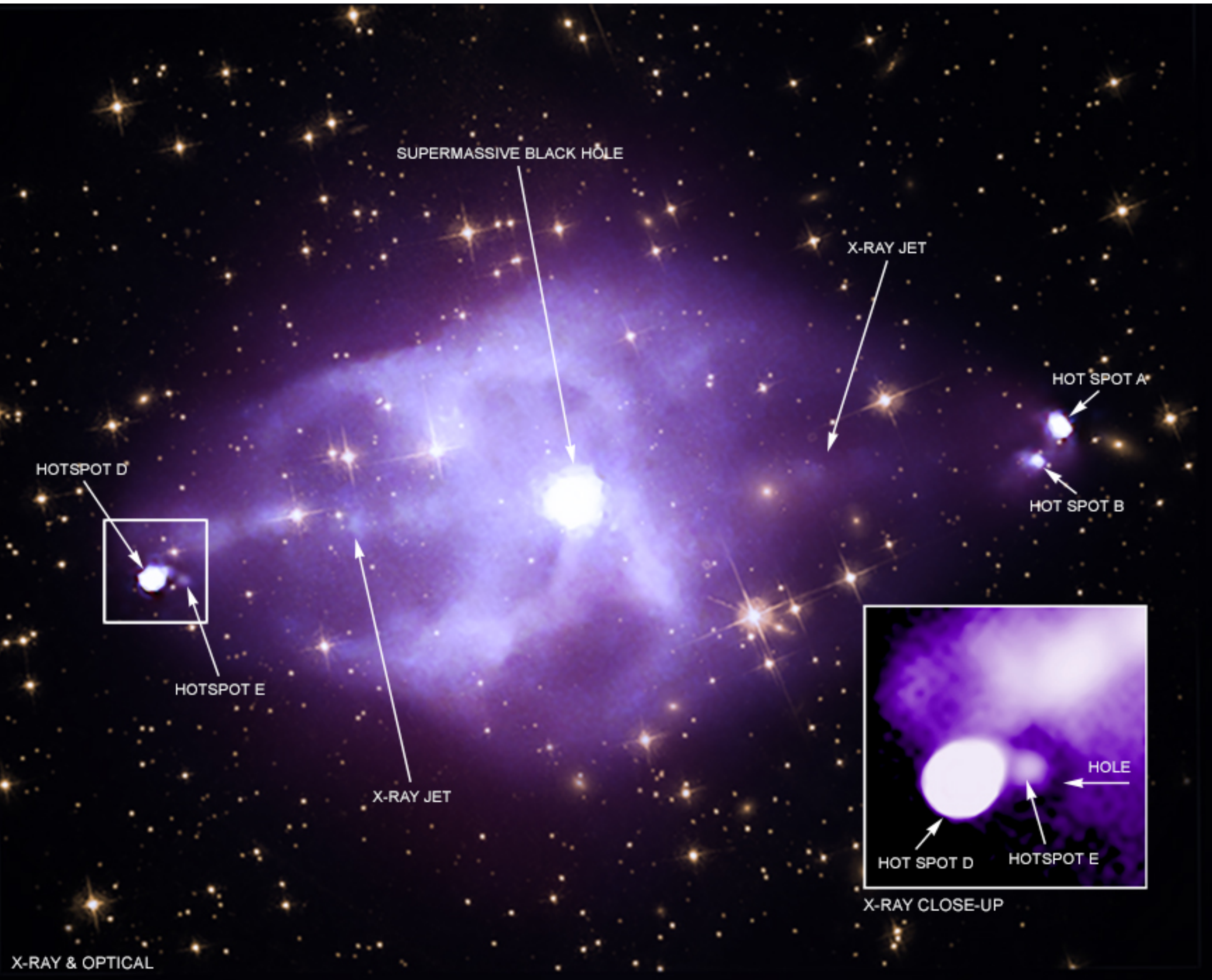
Observations reveal that one of the lobes is connected to the central galaxy of Cyg A by a collimated **jet** that spans the roughly 50h^{-1} kpc of space separating the galaxy from the lobe. (Since the orientations of jets and radio lobes are not well determined, the values for their sizes quoted here are projected distances on the plane of the sky.)

At least half of the stronger radio galaxies have detectable jets, as do more than three-quarters of the weaker sources. The jets associated with the powerful sources tend to be one-sided (like Cyg A's), while those found in less luminous radio galaxies are typically two-sided. One reason for this is that the **stronger radio galaxies can be seen at greater distances, and so a dim counterjet may go undetected.**

Radio lobes and jets

In this composite image of Cygnus A, X-rays from Chandra (red, green, and blue that represent **low, medium and high energy X-rays**) are combined with an optical view from the HST of the galaxies and stars in the same field of view. Chandra's data reveal the presence of **powerful jets of particles and electromagnetic energy** that have shot out from the black hole. The jet on the left has slammed into a **wall of hot gas**, then bounced to **punch a hole** in a cloud of energetic particles, before it **collides with another part of the gas wall**.

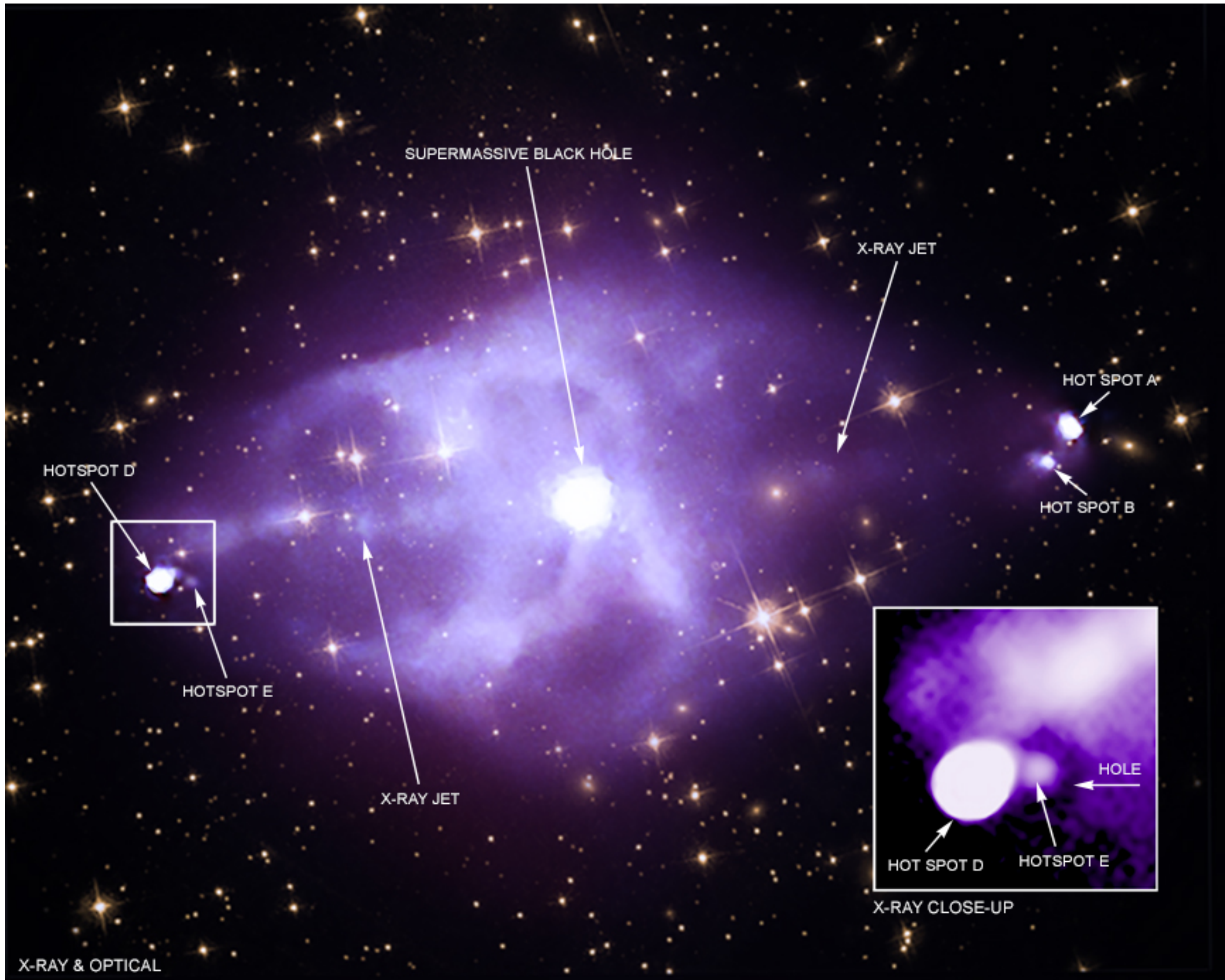
The point that the jet on the left ricocheted off a wall of intergalactic gas ("hotspot E"), and the point where the jet then struck the intergalactic gas a second time ("hotspot D").



Radio lobes and jets

The inset contains a close-up view of the hotspots on the left and the hole punched by the rebounding jet, which surrounds hotspot E. Cygnus A is a large galaxy that sits **in the middle of a cluster of galaxies** about 760 million light years from Earth. Jets can significantly affect how the galaxy and its surroundings evolve.

Energy produced by jets from black holes can **heat intergalactic gas in galaxy clusters and prevent it from cooling** and forming large numbers of stars in a central galaxy like Cygnus A.



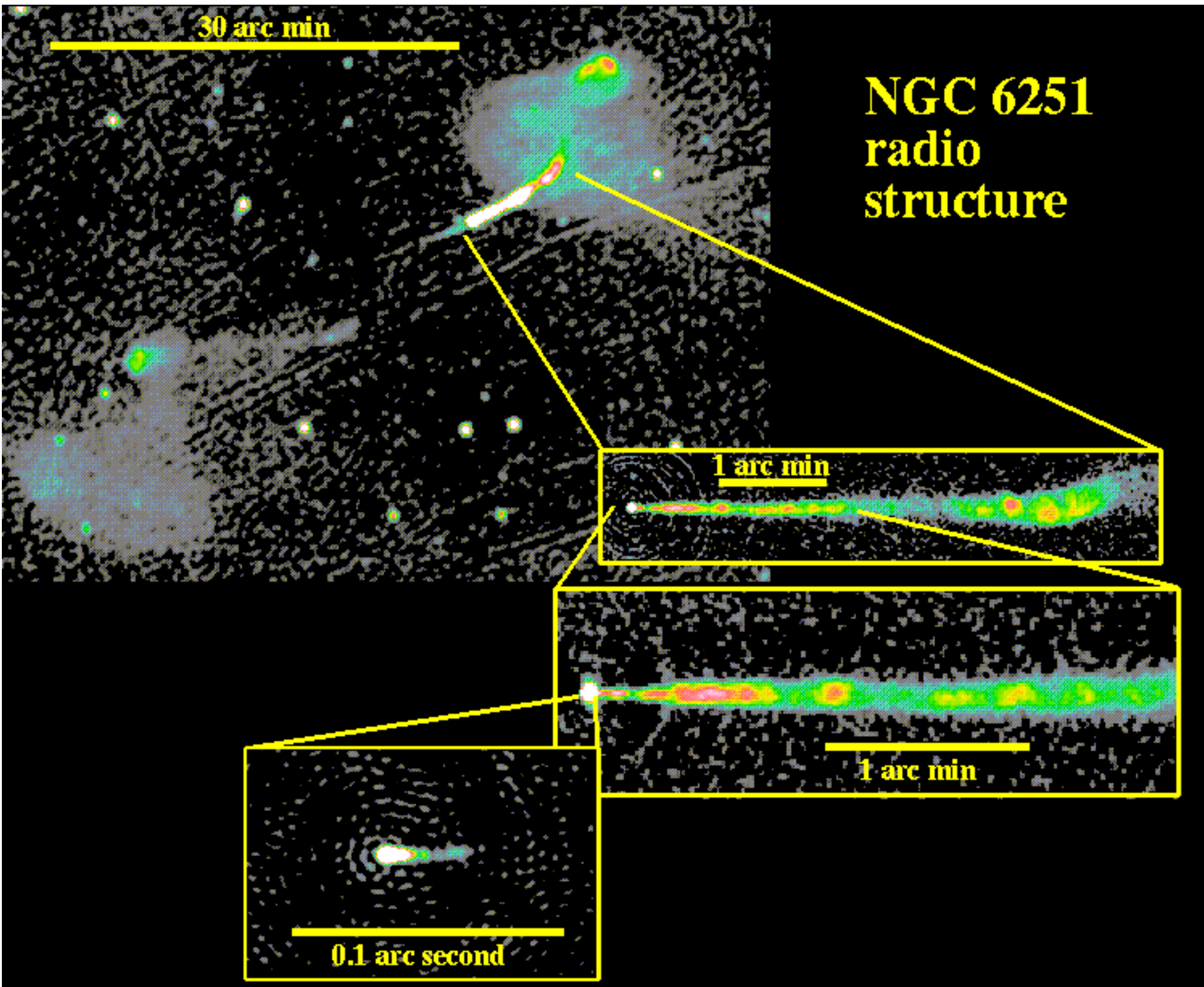
Radio lobes and jets

The strong jet and weak counterjet of the elliptical galaxy NGC 6251.

It is remarkable that the **jet can be traced essentially all the way to the core of the galaxy**.

One important lesson from radio galaxies is that the **central engine continues to eject material in nearly the same direction for at least several million years**, based on the fact that the tiny parsec-scale jets in the core regions point in the same direction as the very extended radio structure which may stretch several million light-years (and thus took at least that many years to form).

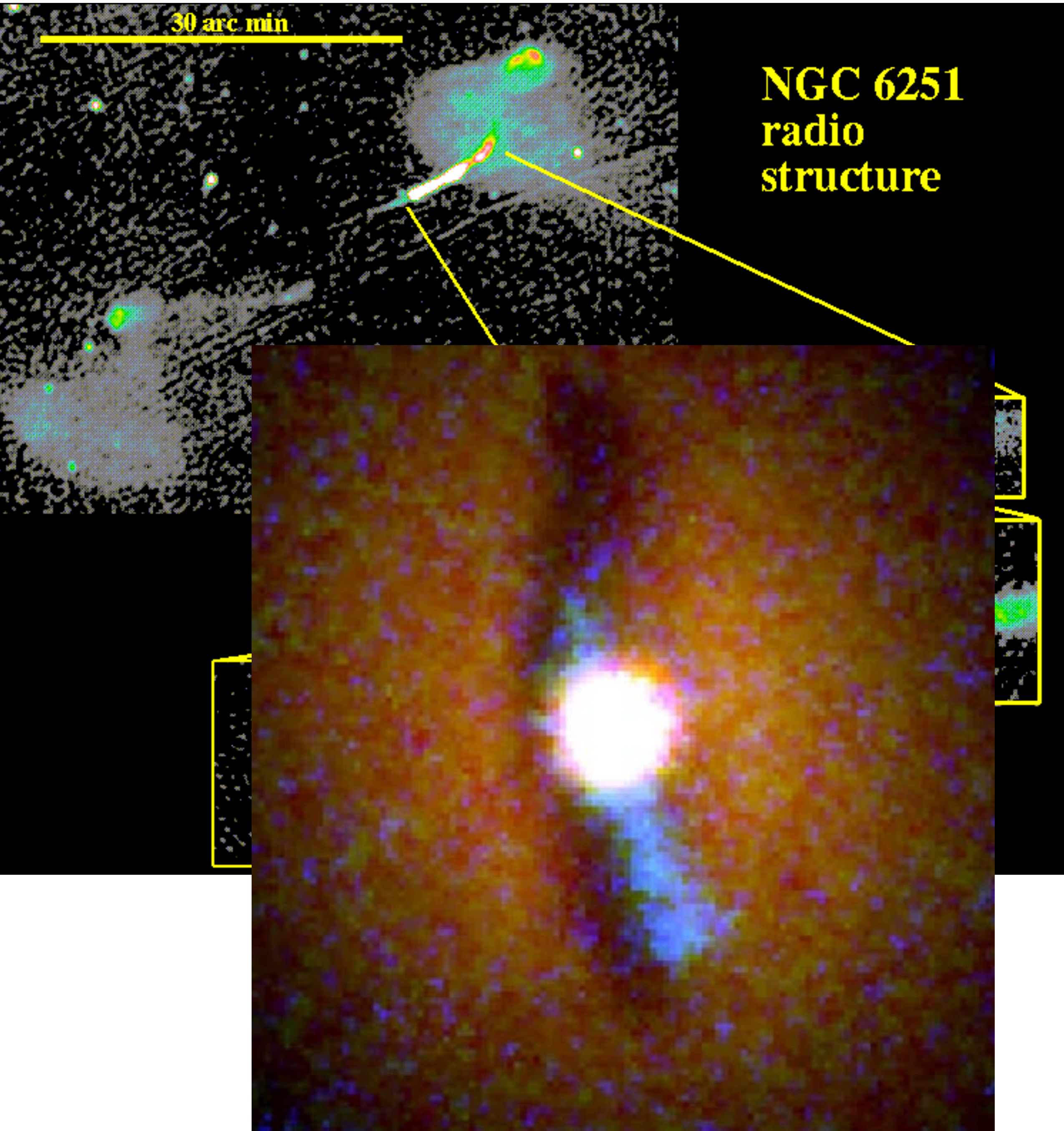
The WSRT map shows the faint counterjet opposite the bright jet; its weakness may indicate that the jet is in relativistic motion more or less toward us, so that **Doppler boosting** makes it appear dramatically brighter than its counterpart.



Radio lobes and jets

Something is lighting up the centre of galaxy NGC 6251. Most likely a large black hole not shrouded by gas and dust typically found near the centre of a galaxy.

Observations taken with the Hubble Space Telescope indicate a new perspective on the centres of galaxies: a **bright central object that is illuminating a surrounding material disk**, shown in blue. The lack of reflection from the upper part of the disk indicates that this **disk is warped in shape**. A huge plasma jet streams out from the central object, perpendicular to the warped disk.



Radio lobes and jets

Other radio jets are not as straight as those of Cyg A or **NGC 6251**.

The windblown appearance of the jets emanating from NGC 1265, produced by that galaxy's motion through the intracluster gas of the **Perseus cluster**.

Galaxy clusters tend to host the **largest elliptical galaxies**. Due to the galaxy density in clusters **interactions and mergers are very frequent** between the galaxies -> **giant elliptical galaxies can form**.

Most galaxy clusters have a giant elliptical galaxy in the centre of the cluster.

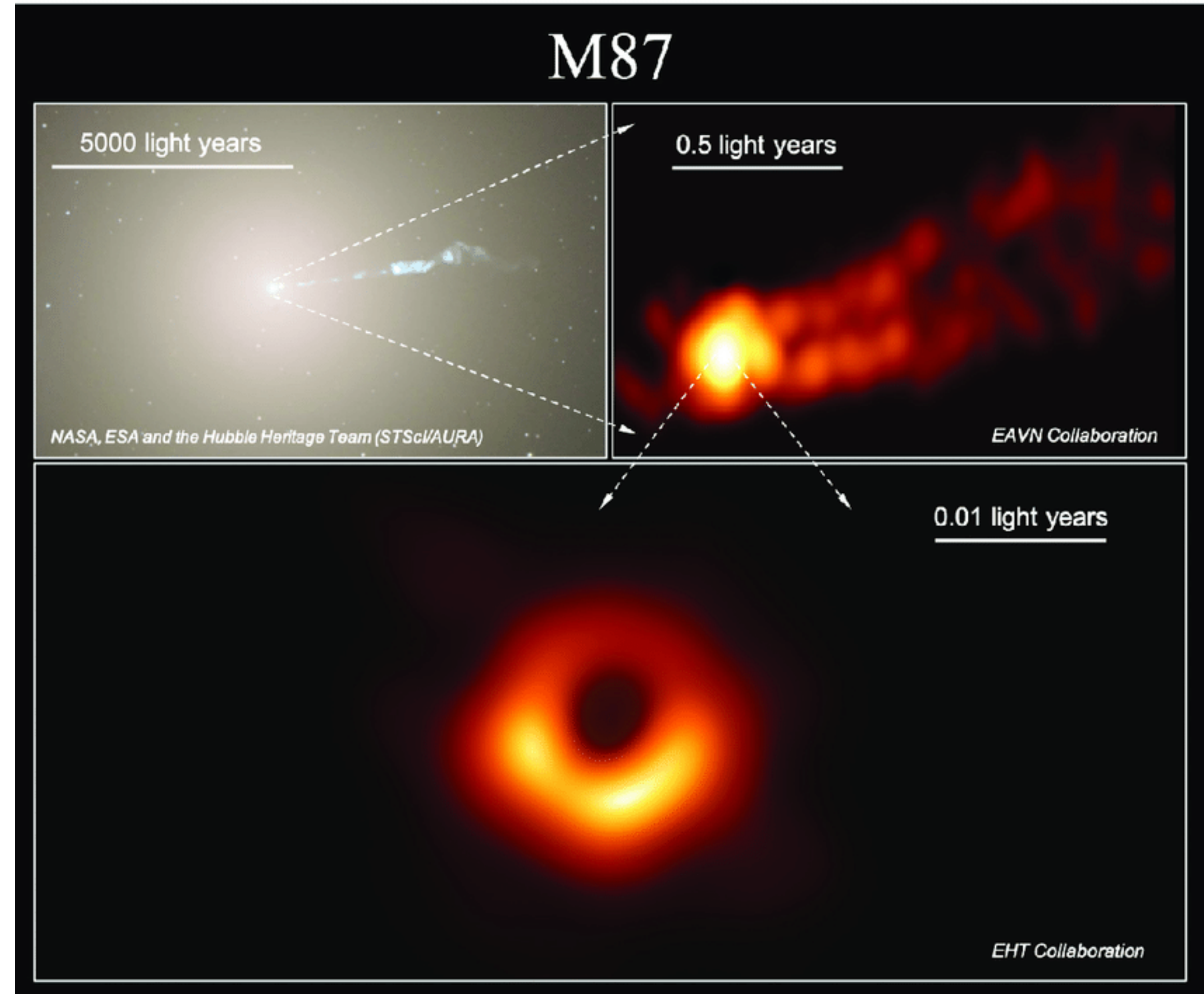


Radio lobes and jets

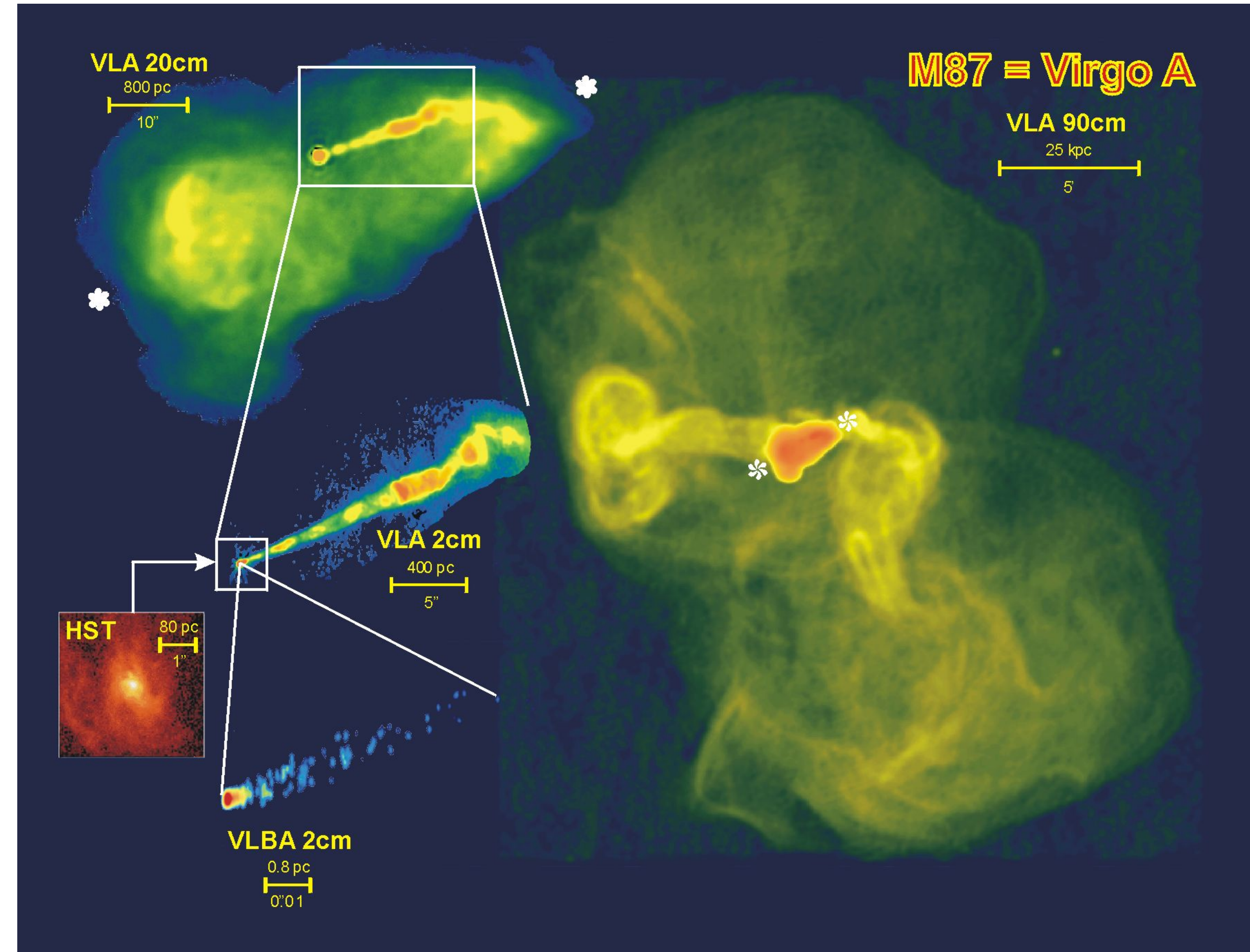
Following Cyg A, many more radio galaxies were discovered. One of these is M87, the **giant elliptical (E1)** galaxy that lies at the **center of the Virgo cluster**. With an apparent visual magnitude of $V = 8.7$, M87 is **one of the brighter-appearing galaxies in the sky**.

The **Virgo cluster** is the **closes galaxy cluster** to us.

HST view of M87, also known as Virgo A to radio astronomers. Its prominent jet, shown at the right, was discovered optically in 1917. The jet extends from the galaxy some 1.5 kpc into one of its radio lobes.



Radio lobes and jets

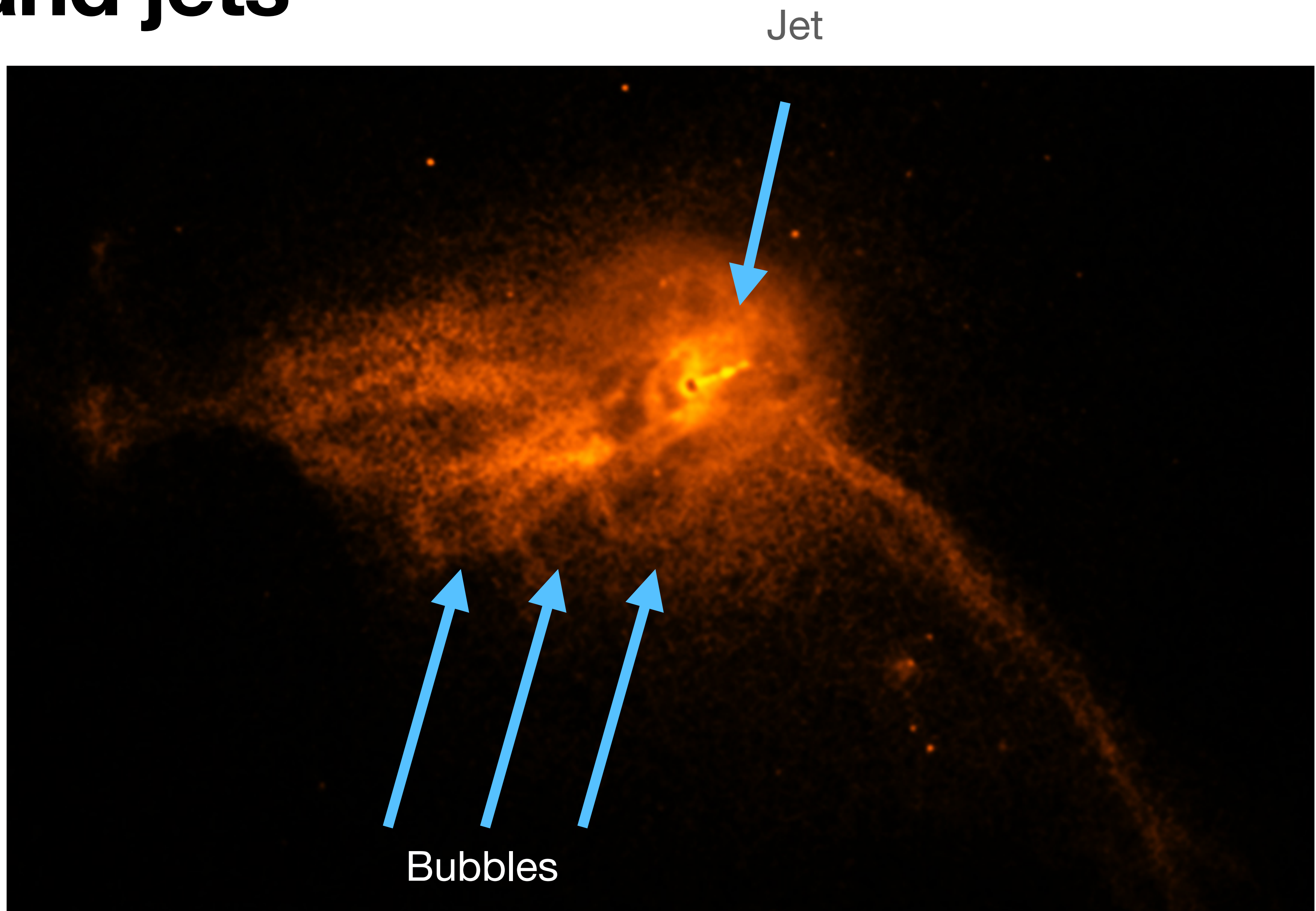


Large scale radio structure of M87.

Radio lobes and jets

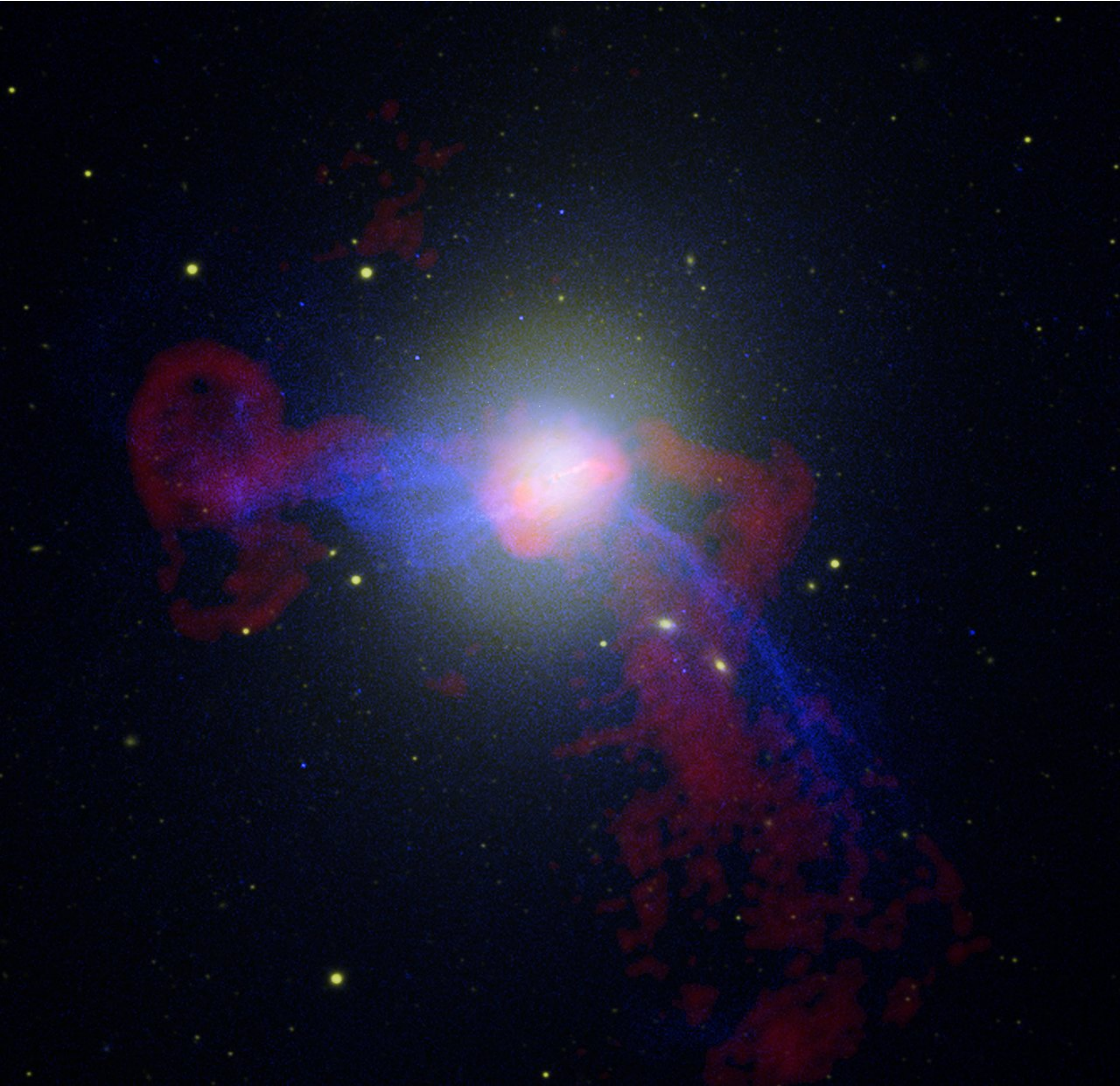
The jet also displays evenly spaced **knots** that are bright at radio, visible, and **X-ray wavelengths**. The X-ray luminosity of M87, including the jet, is roughly 10^{36} W. This is about 50 times greater than M87's radio luminosity.

There is also evidence for a **faint counterjet** extending away from M87 in the direction opposite that of the dominant jet.



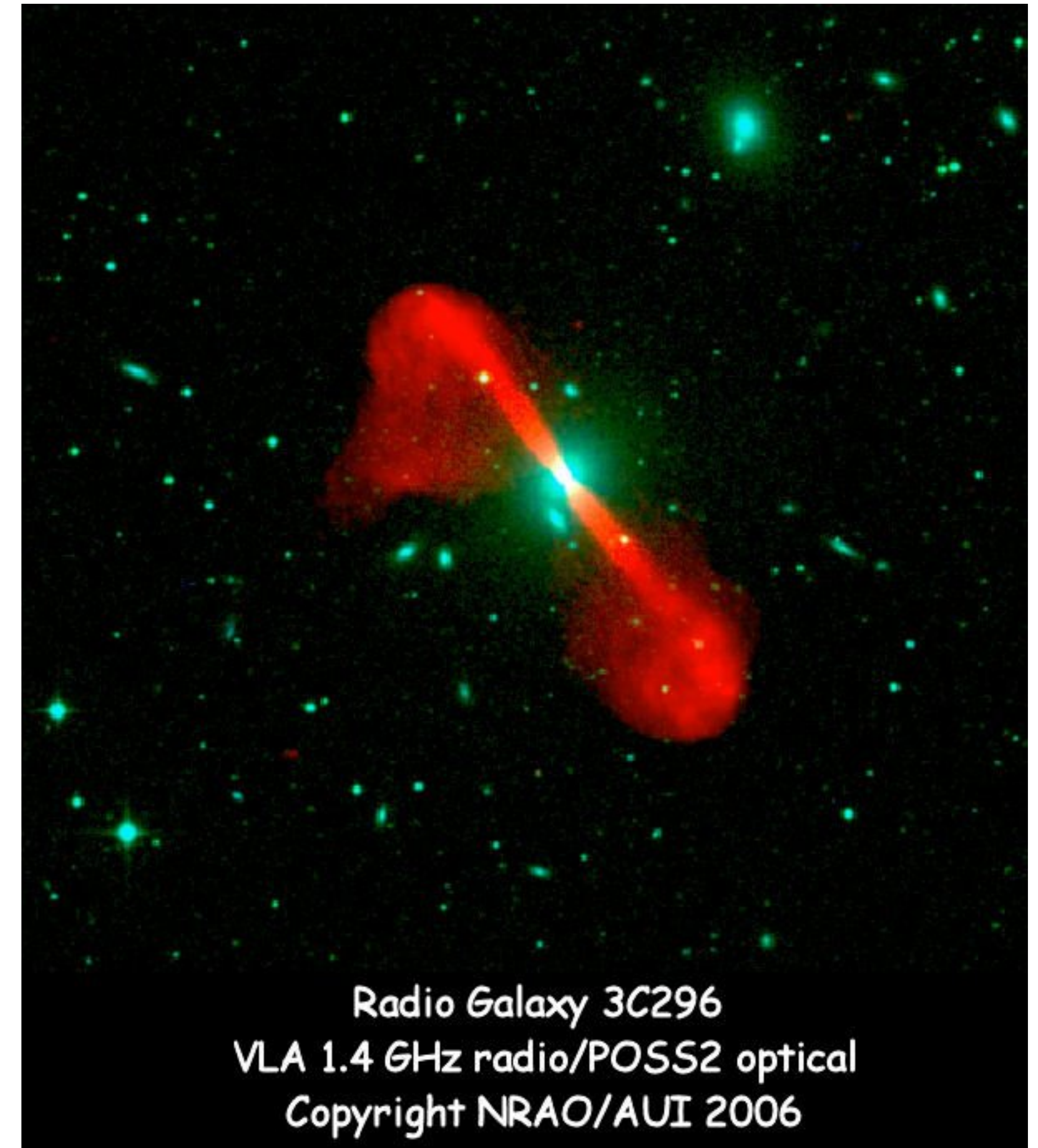
Radio lobes and jets

Radio - red
X-ray - blue
Optical - green



Radio lobes and jets

One of the largest radio galaxies known is 3C 236 (the “3C” designates a listing in the **Third Cambridge Catalog** of radio sources). With a redshift of $z = 0.0988$, its distance is about $280h^{-1}$ Mpc, according to Hubble’s law. The radio lobes of 3C 236 are separated by more than $1.5h^{-1}$ Mpc, projected onto the plane of the sky, while its radio jet is only $400h^{-1}$ pc long.

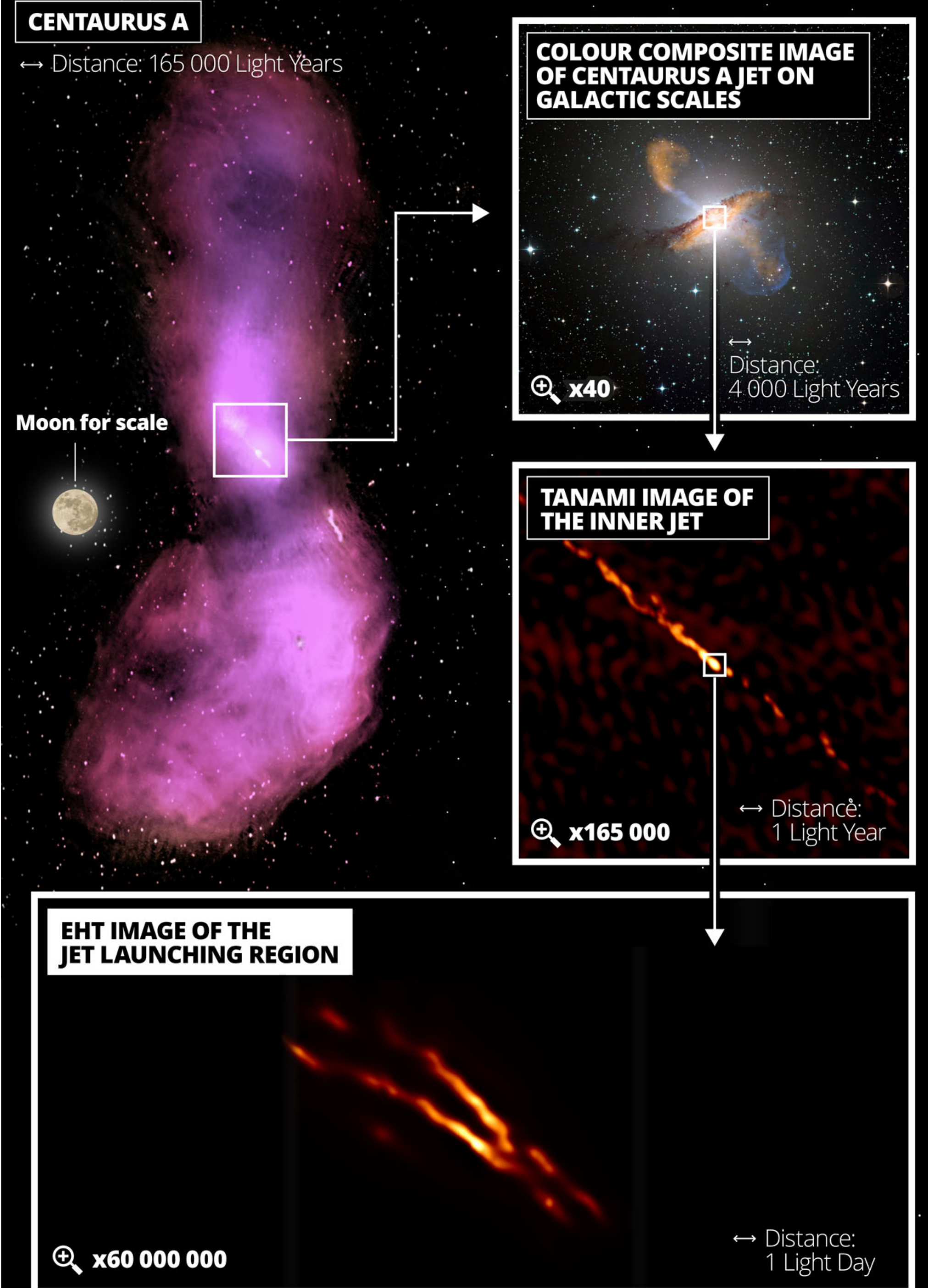


Radio Galaxy 3C296
VLA 1.4 GHz radio/POSS2 optical
Copyright NRAO/AUI 2006

Radio lobes and jets

The closest example of an AGN is **Centaurus A** (NGC 5128), at a distance of $4.7 h^{-1}$ Mpc.

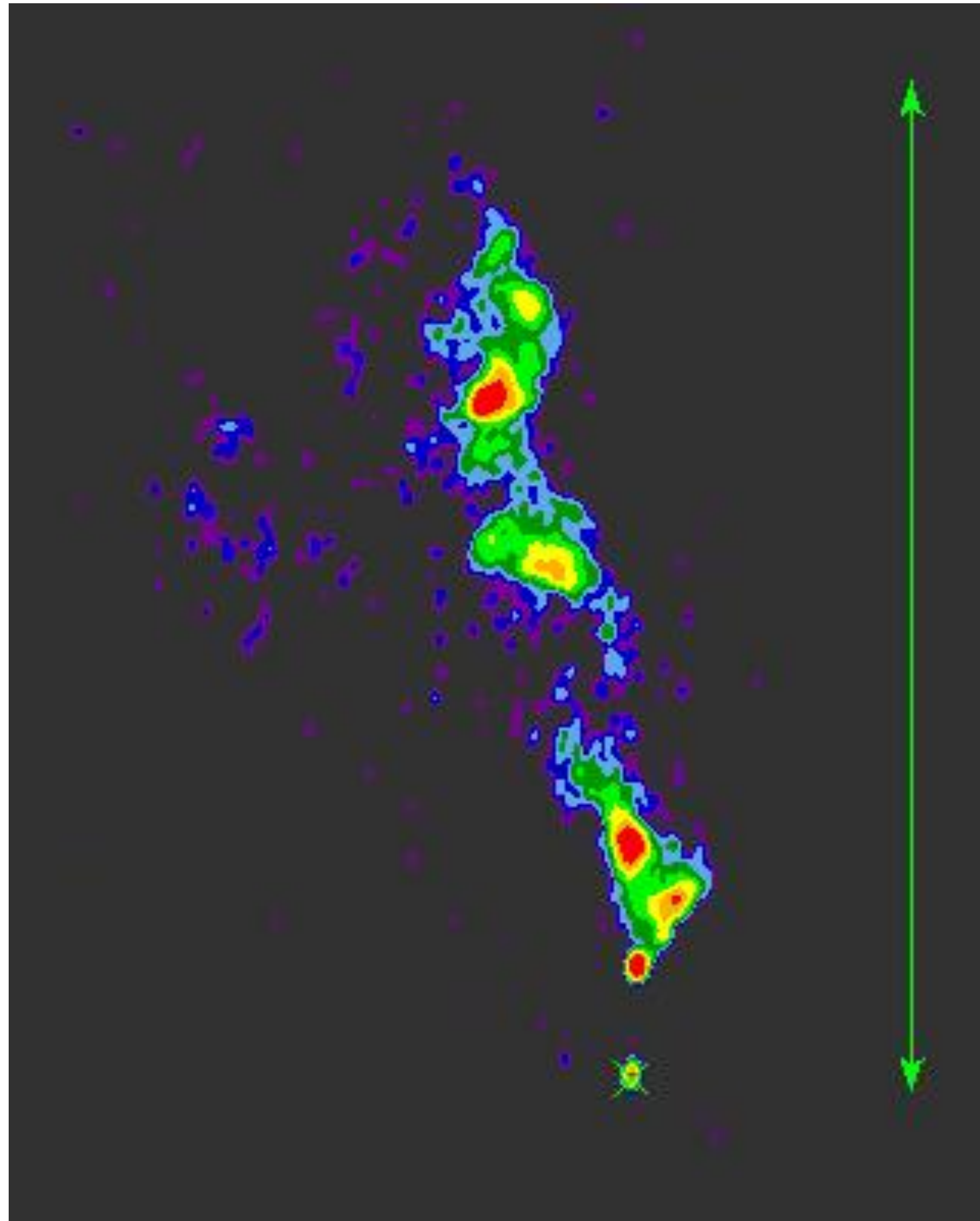
An E2 galaxy girded by a thick dust lane. Superimposed on the photograph is a radio map showing the radio lobes. Like M87, Cen A has a jet extending from its nucleus containing several knots of radio and X-ray emission. Although Cen A is in our astronomical backyard, radio galaxies on average are roughly 100 times less abundant than Seyferts in regions that are nearby in cosmological terms.



Quasars

3C 48 VLBA image (very high angular resolution)

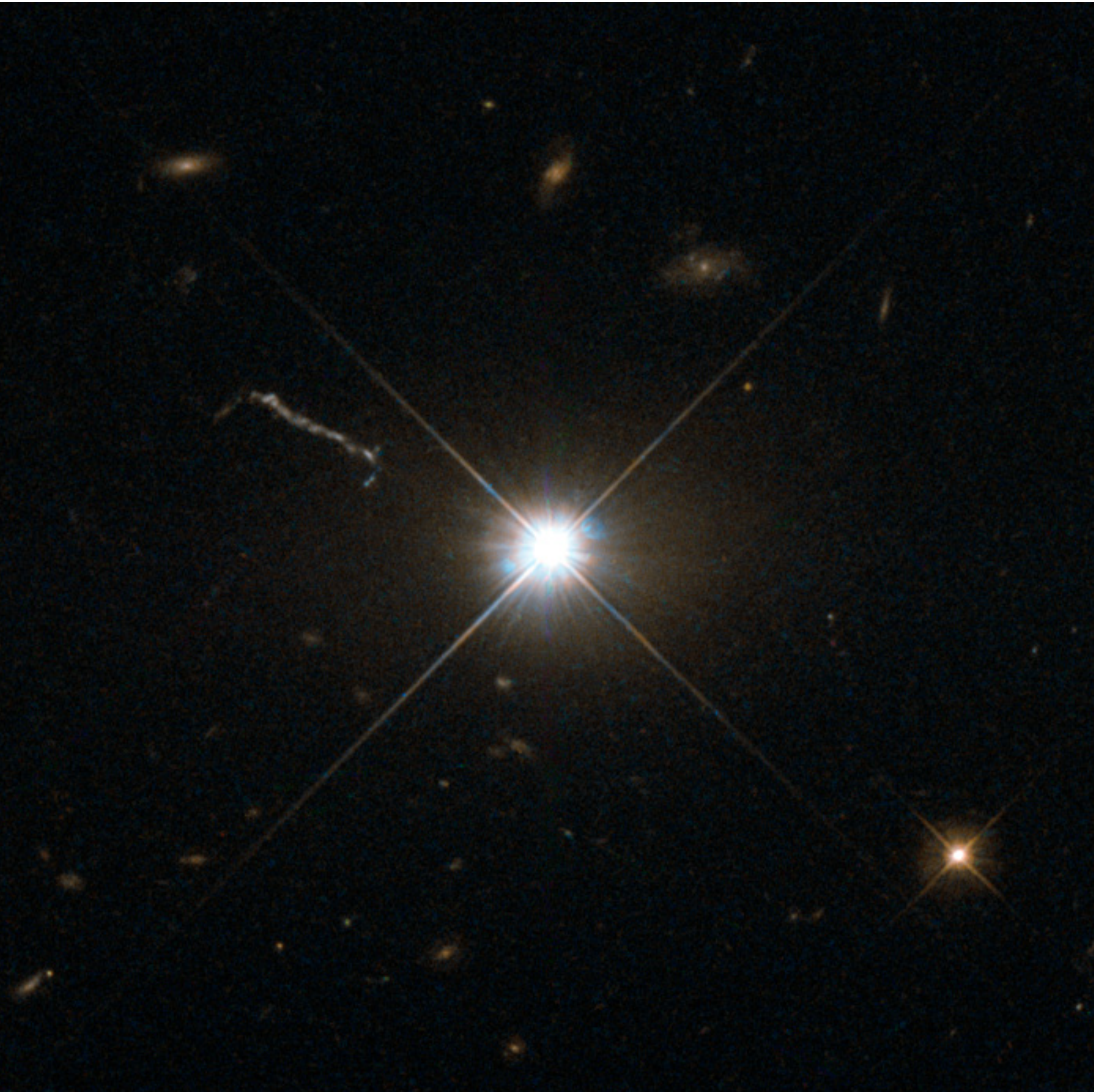
As radio telescopes discovered **increasing numbers of radio sources** in the late 1950s, the task of **identifying these** sources with known objects became more important. In 1960 Thomas Matthews and Allan Sandage were searching for an optical counterpart to another radio source, 3C 48. They found a 16th-magnitude **starlike object** whose unique spectrum displayed **broad emission lines** that could not be identified with any known element or molecule.



Quasars

3C 273 - Hubble image

In 1963 a similarly weird spectrum was found for **another radio source with a stellar appearance**, 3C 273. Figure 12 shows 3C 273 and its jet, which extends a projected distance of $39h^{-1}$ kpc from the nucleus.



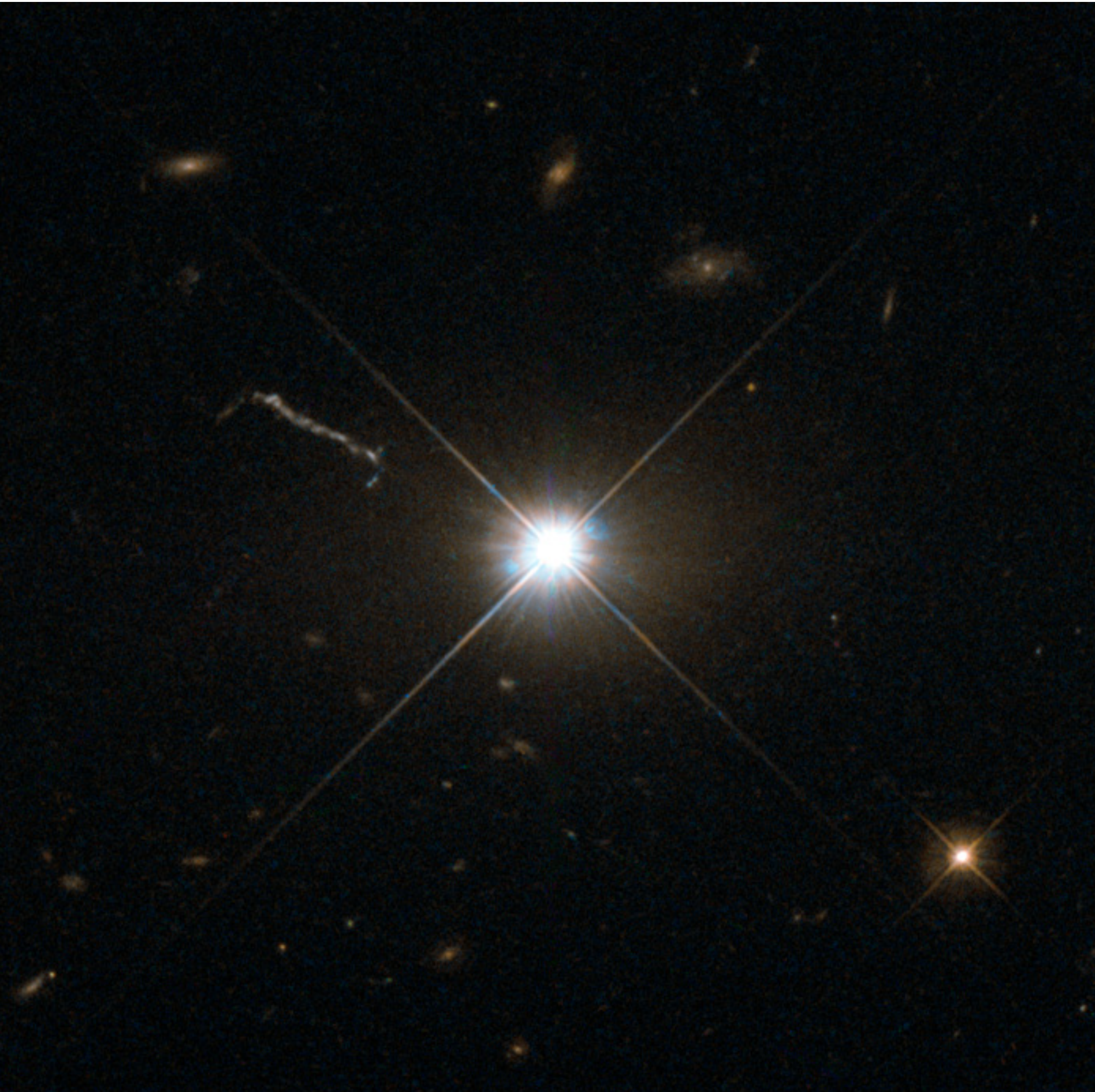
Quasars

3C 273 - Hubble image

In 1963 a similarly weird spectrum was found for **another radio source with a stellar appearance**, 3C 273. Figure 12 shows 3C 273 and its jet, which extends a projected distance of $39h^{-1}$ kpc from the nucleus.

3C 48, 3C 273, and other, similar sources were classified as **quasi-stellar radio sources (QSRs)**, which became known as **quasars**.

Later, the mystery lifted somewhat when astronomers recognized that the pattern of the broad emission lines of 3C 273 was the same as the pattern of the **Balmer lines of hydrogen**. These lines had been **severely redshifted** ($z = 0.158$), making their identification difficult. According to Hubble's law, this places 3C 273 at a distance of about $440h^{-1}$ Mpc.



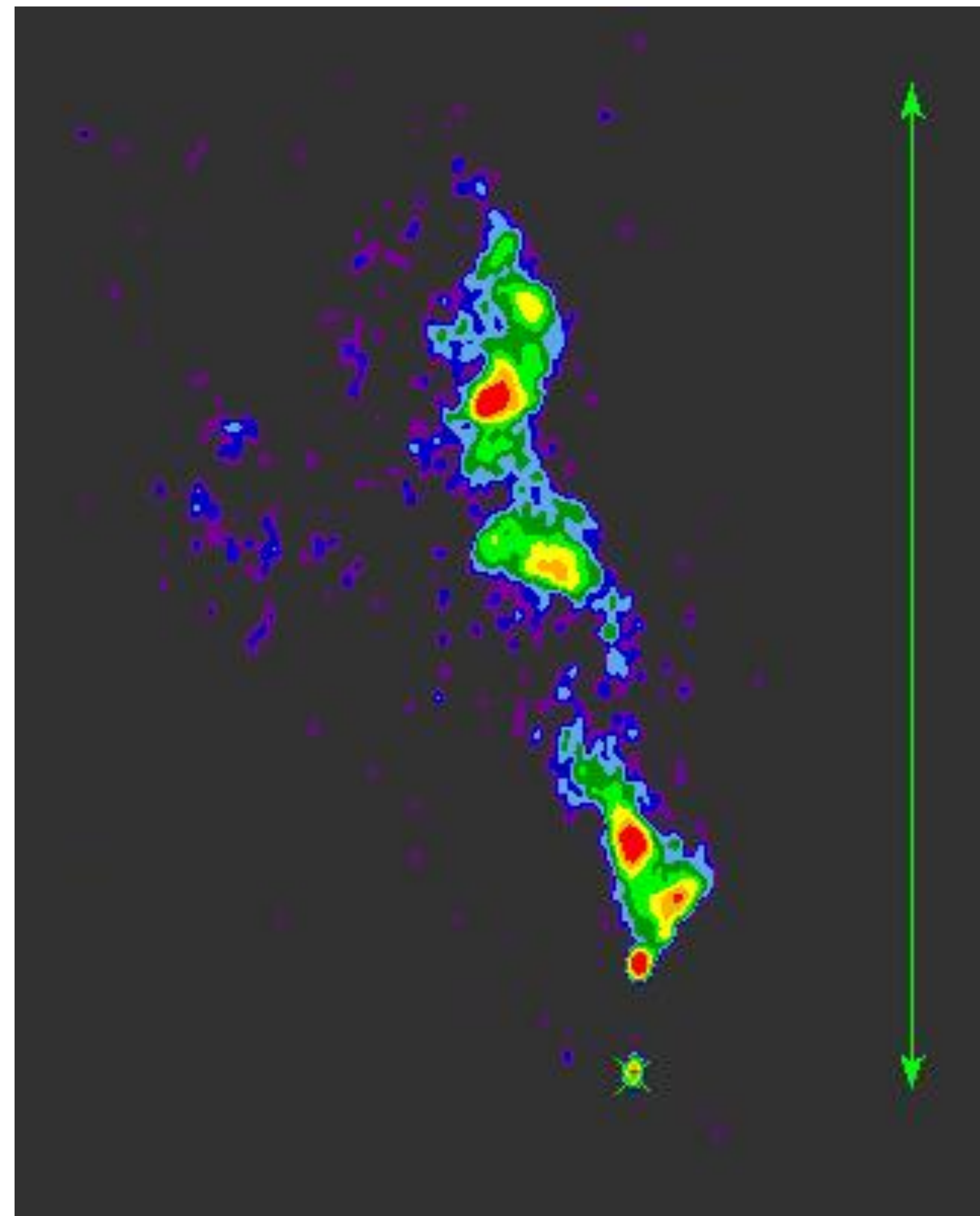
Quasars

3C 48 VLBA image (very high angular resolution)

3C 48 has an even greater redshift, $z = 0.367$, corresponding to a radial velocity of $0.303c$ and a Hubble distance of just over $900h^{-1}$ Mpc.

Astronomers realized that **3C 48 was one of the most distant objects yet discovered** in the universe.

Today we have discovered many more even more distant quasars.



Quasars

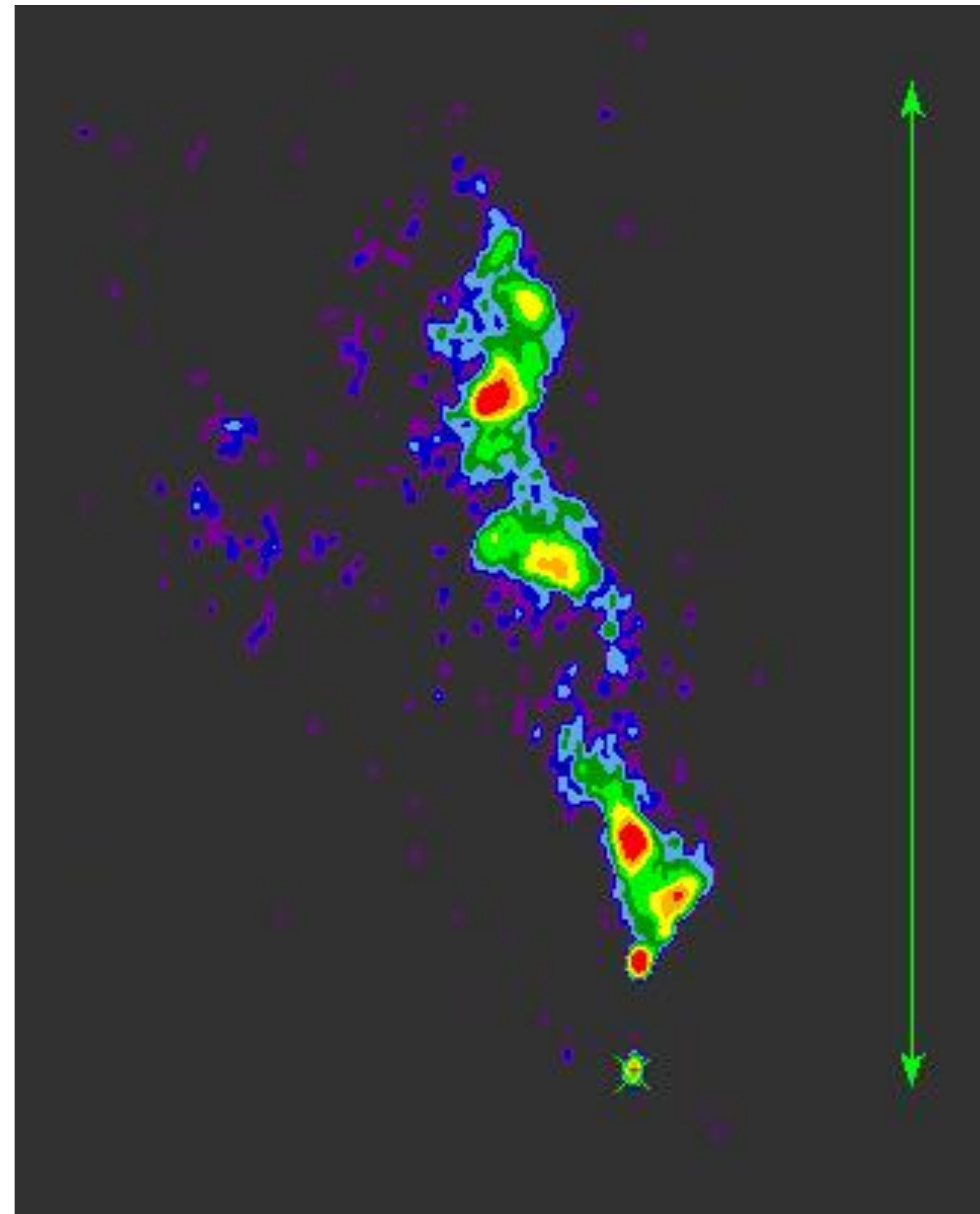
3C 48 VLBA image (very high angular resolution)

3C 48 has an even greater redshift, $z = 0.367$, corresponding to a radial velocity of $0.303c$ and a Hubble distance of just over $900h^{-1}$ Mpc.

3C 48 was one of the most distant objects yet discovered (at the time of the first redshift measurement).

Today the most distant quasars are around $z = \sim 7.6$ and the James Webb telescope is finding objects at $z = \sim 13$.

A quasar's radio emission may come either from radio lobes or from a central source in its core. Quasars are so far away that in optical images most appear as overwhelmingly bright, starlike nuclei surrounded by faint fuzzy halos. In some cases, a fuzzy halo can be resolved into a faint parent galaxy. **To be visible from such great distances, quasars must be exceptionally powerful.**



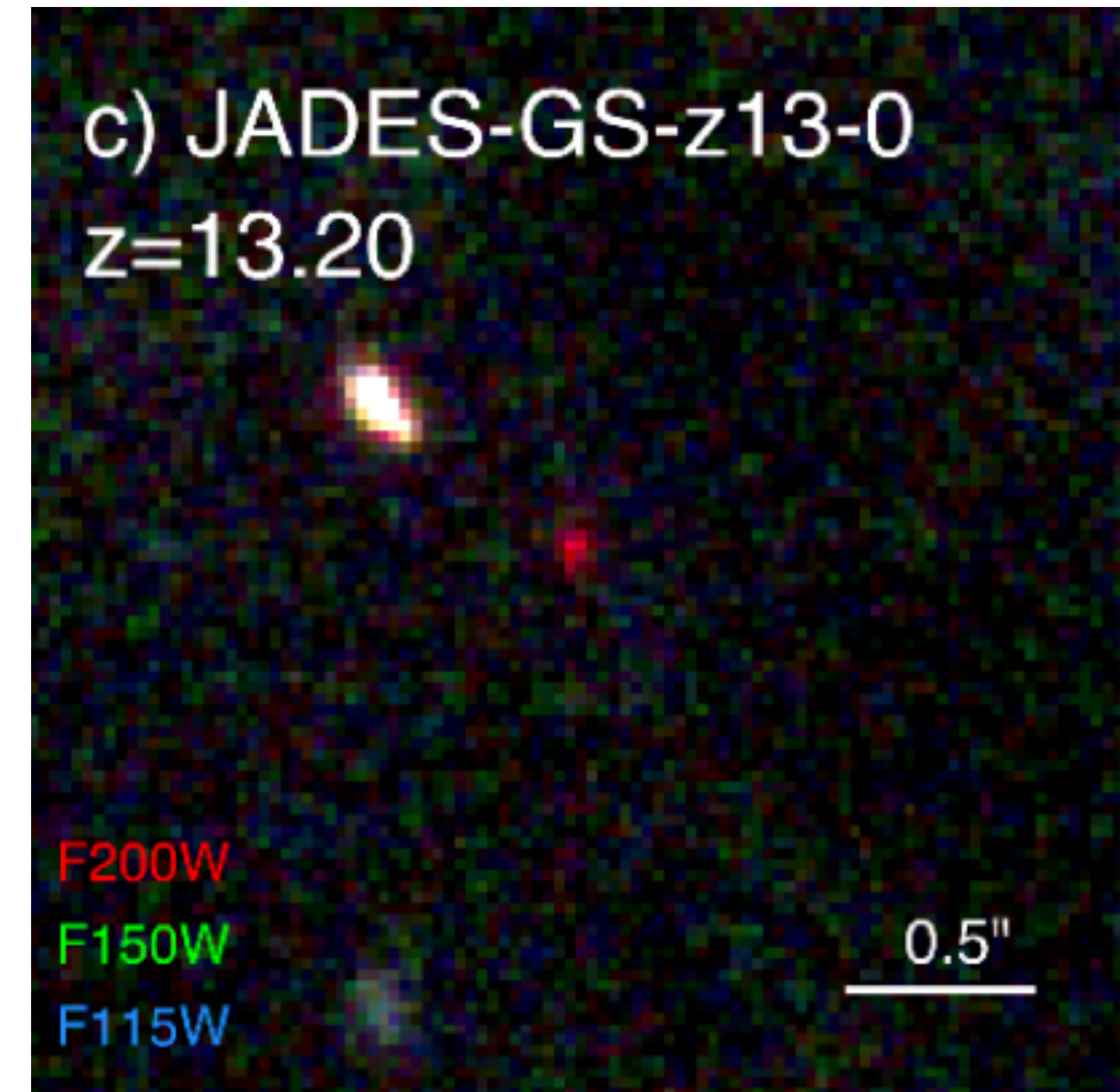
Quasars

This object was detected with the James Webb telescope and has an approximate redshift of $z = 13.20$ (redshift is determined with spectroscopy). The **age of the Universe is estimated to be $z = 13.787$**

Identified as a Lyman-break galaxy. **Lyman-break galaxies are star-forming galaxies at high redshift** that are selected using the differing appearance of the galaxy in several **imaging filters** due to the position of the Lyman limit.

Radiation at higher energies than the Lyman limit at 912 Å is almost completely absorbed by neutral gas around star-forming regions of galaxies. In the rest frame of the emitting galaxy, the emitted spectrum is bright at wavelengths longer than 912 Å, but very dim or imperceptible at shorter wavelengths — this is known as a "dropout", or "break", and can be used to find the position of the Lyman limit. At high redshift galaxies this break is shifted to optical or infrared wavelengths.

The most distant object in the Universe? In 2023.



Quasars

Example 1.2. The following equation can be used to obtain the absolute visual magnitude of the quasar 3C 273, which has an apparent visual magnitude of $V = 12.8$:

$$m - M = 5 \log_{10}(d) - 5 = 5 \log_{10} \left(\frac{d}{10 \text{ pc}} \right).$$

Adopting $[h]_{\text{WMAP}} = 0.71$ yields a distance of $d \approx 620 \text{ Mpc}$, implying that

$$M_V = V - 5 \log_{10} \left(\frac{d}{10 \text{ pc}} \right) = -26.2.$$

This value can be used to obtain an estimate of the luminosity of the quasar at visual wavelengths. Using $M_{\text{Sun}} = 4.82$ for the Sun's absolute visual magnitude gives an **estimate of the quasar's visual luminosity**:

$$L_V \approx 100^{(M_{\text{Sun}} - M_V)/5} L_{\odot} = 2.6 \times 10^{12} L_{\odot} = 1 \times 10^{39} \text{ W}.$$

Quasars

The radio energy emitted by 3C 273 can be estimated from its distance and the value of the monochromatic flux at a radio frequency of 1400 MHz, $F_{1400} = 4.64 \times 10^{-25} \text{ W m}^{-2} \text{ Hz}^{-1} = 46.4 \text{ Jy}$. The radio spectrum follows the power law with a spectral index of $\alpha \approx 0.24$. Integrating the monochromatic flux from $\nu_1 \approx 0$ to $\nu_2 = 3 \text{ GHz}$ gives

$$L_{\text{radio}} = 4\pi d^2 \int_{\nu_1}^{\nu_2} F_{\nu} d\nu = 7 \times 10^{36} \text{ W}.$$

The bolometric luminosities inferred for quasars range from about 10^{38} W to more than 10^{41} W , with $5 \times 10^{39} \text{ W}$ being a typical value.

This implies that the most luminous quasars are on the order of **10⁵ times more energetic than a normal galaxy like our own Milky Way**.

Quasar spectra

The monochromatic flux of 3C 273 is shown in Fig. 14.

This continuous spectrum spans nearly **15 orders of magnitude in frequency**, very broad compared with the sharply peaked blackbody spectrum of a star.

The **decline at the low-frequency end** of the spectrum reflects the larger-than-average spectral index ($\alpha = 0.24$) for 3C 273 in this regime.

->At **low frequencies**, the spectrum is **dominated by radiation from its jet**.

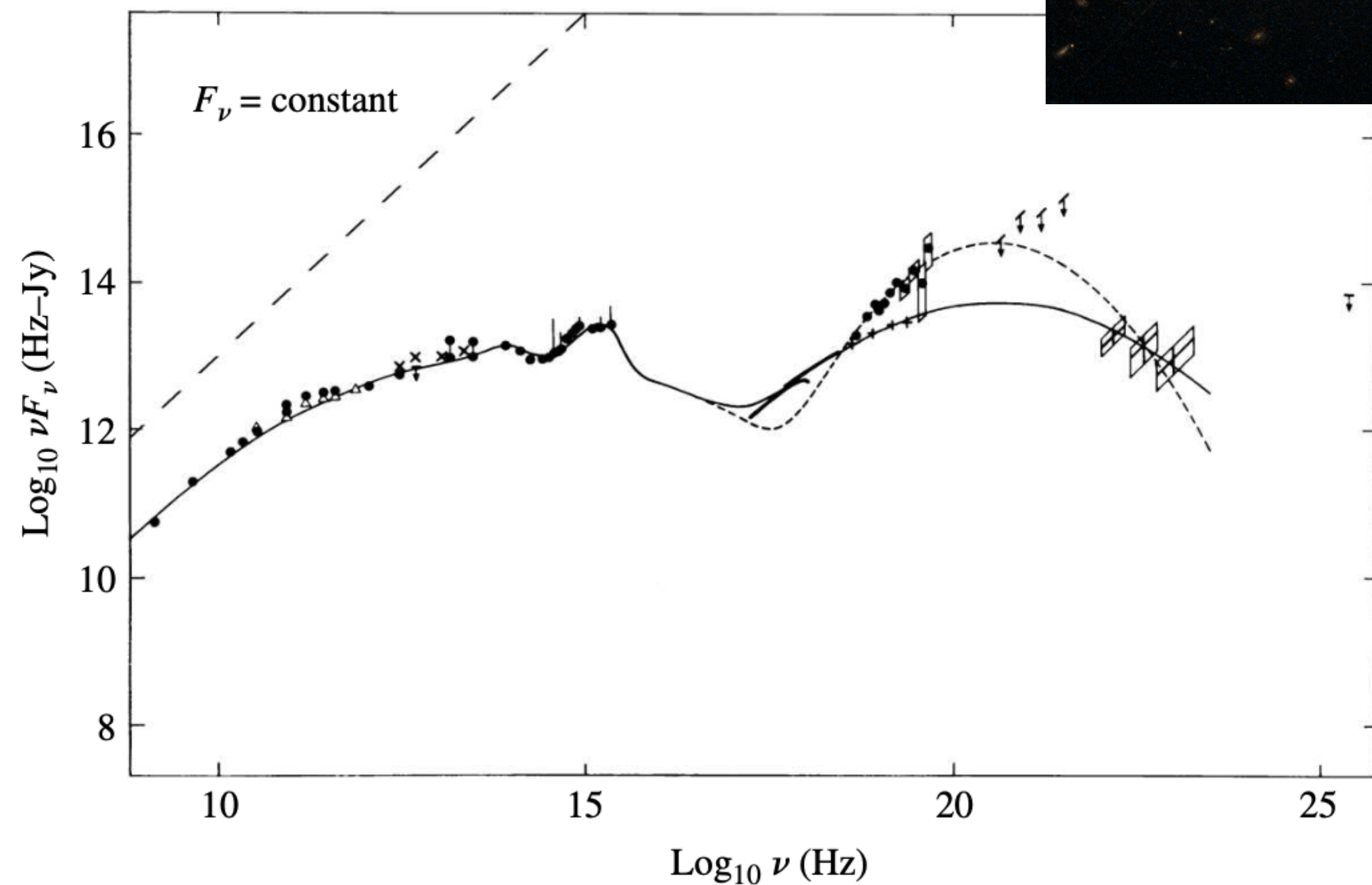
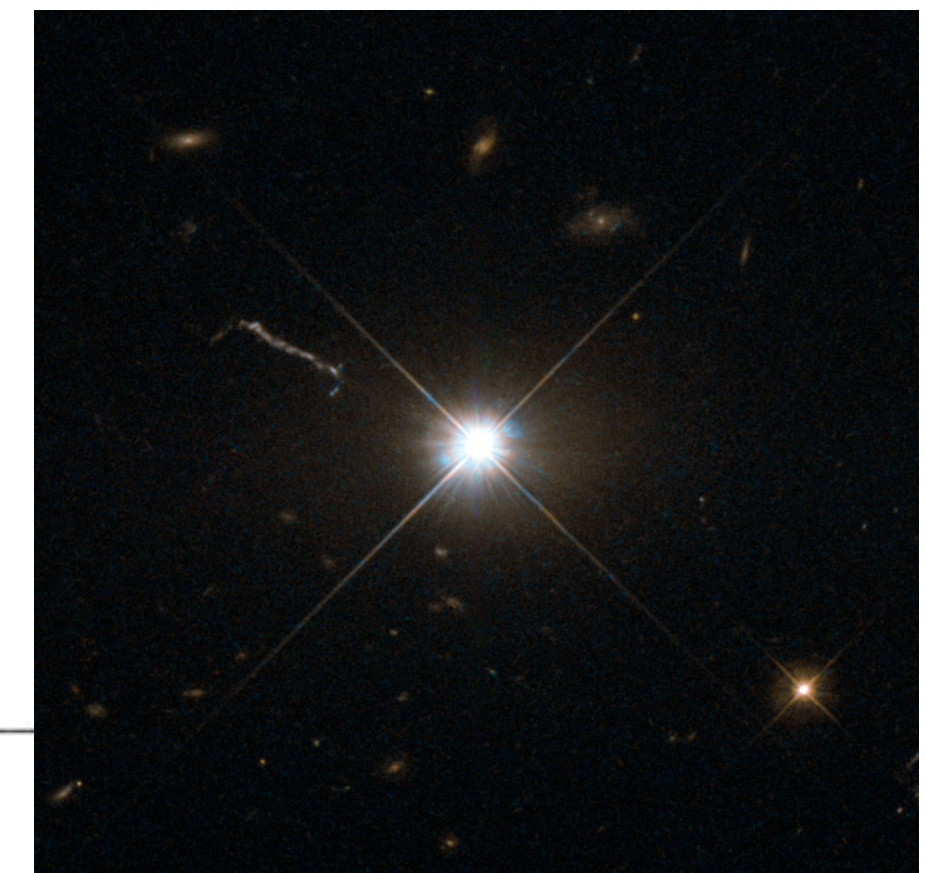


FIGURE 14 The spectrum of 3C 273, after the Doppler shift of the frequencies due to the Hubble flow has been removed. A horizontal line would correspond to a spectral index of $\alpha = 1$; for reference, the diagonal dashed line shows the slope for $F_\nu = \text{constant}$. The two lines on the right correspond to 3C 273 during quiescence and during an outburst. (Figure adapted from Perry, Ward, and Jones, *MNRAS*, 228, 623, 1987.)



Quasar spectra

For **most other quasars**, the spectrum at the low-frequency end falls off more abruptly (**smaller α**). A **typical spectrum turns over in the far infrared** at a frequency of about 5×10^{12} Hz, possibly due to dust and/or synchrotron self-absorption.

Some quasars are most luminous at infrared wavelengths and others peak in **X-rays**.

The peak power output of **3C 273** is in the form of low-energy **gamma rays**.

Quasars emit an excess of **ultraviolet light** relative to stars and so are quite blue in appearance.

In Fig. 14, this ultraviolet excess is indicated by the big **blue bump** between roughly 10^{14} Hz and 10^{16} Hz. A big blue bump is a feature of most (but not all) quasar spectra.

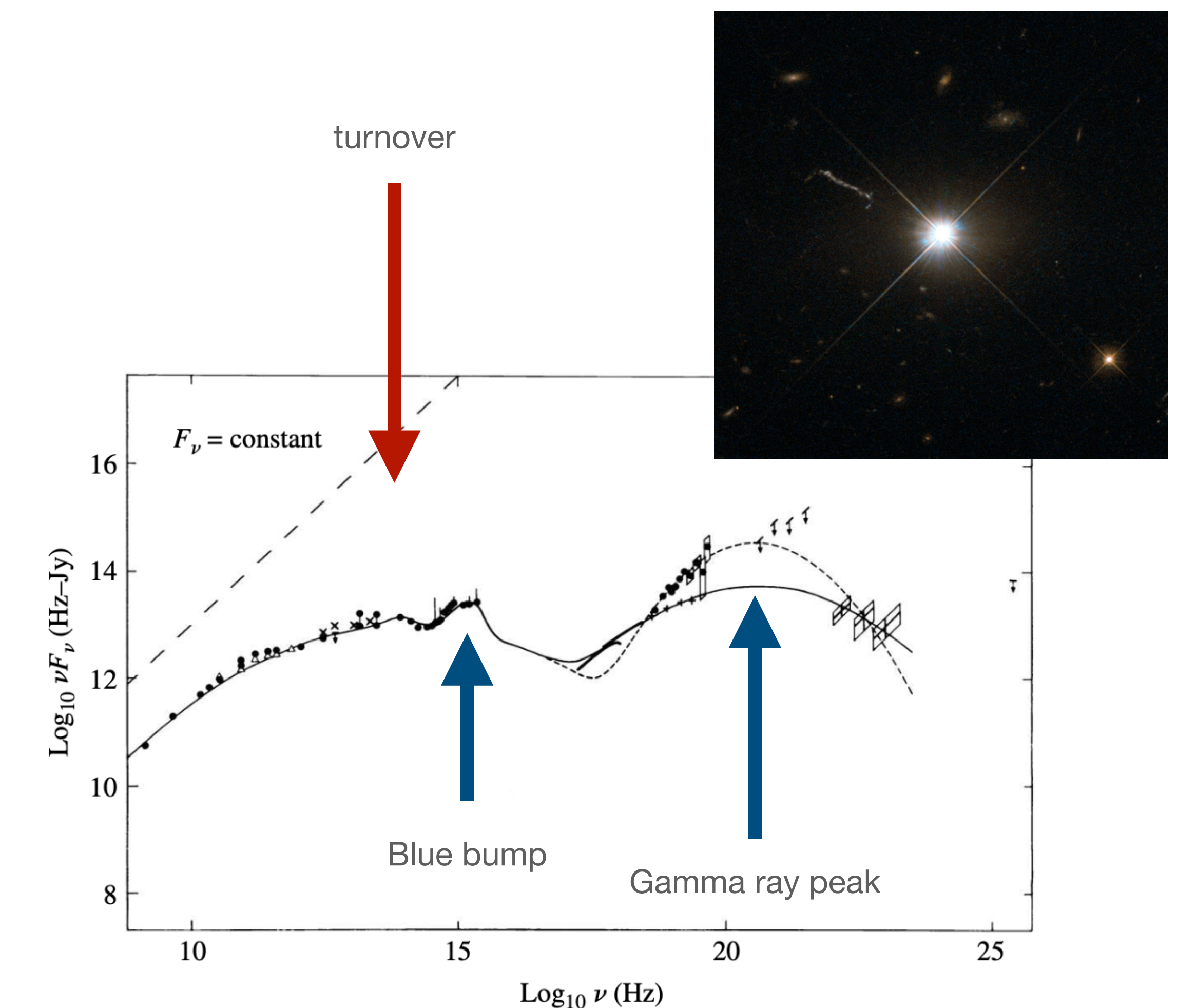


FIGURE 14 The spectrum of 3C 273, after the Doppler shift of the frequencies due to the Hubble flow has been removed. A horizontal line would correspond to a spectral index of $\alpha = 1$; for reference, the diagonal dashed line shows the slope for $F_\nu = \text{constant}$. The two lines on the right correspond to 3C 273 during quiescence and during an outburst. (Figure adapted from Perry, Ward, and Jones, *MNRAS*, 228, 623, 1987.)

Quasar spectra

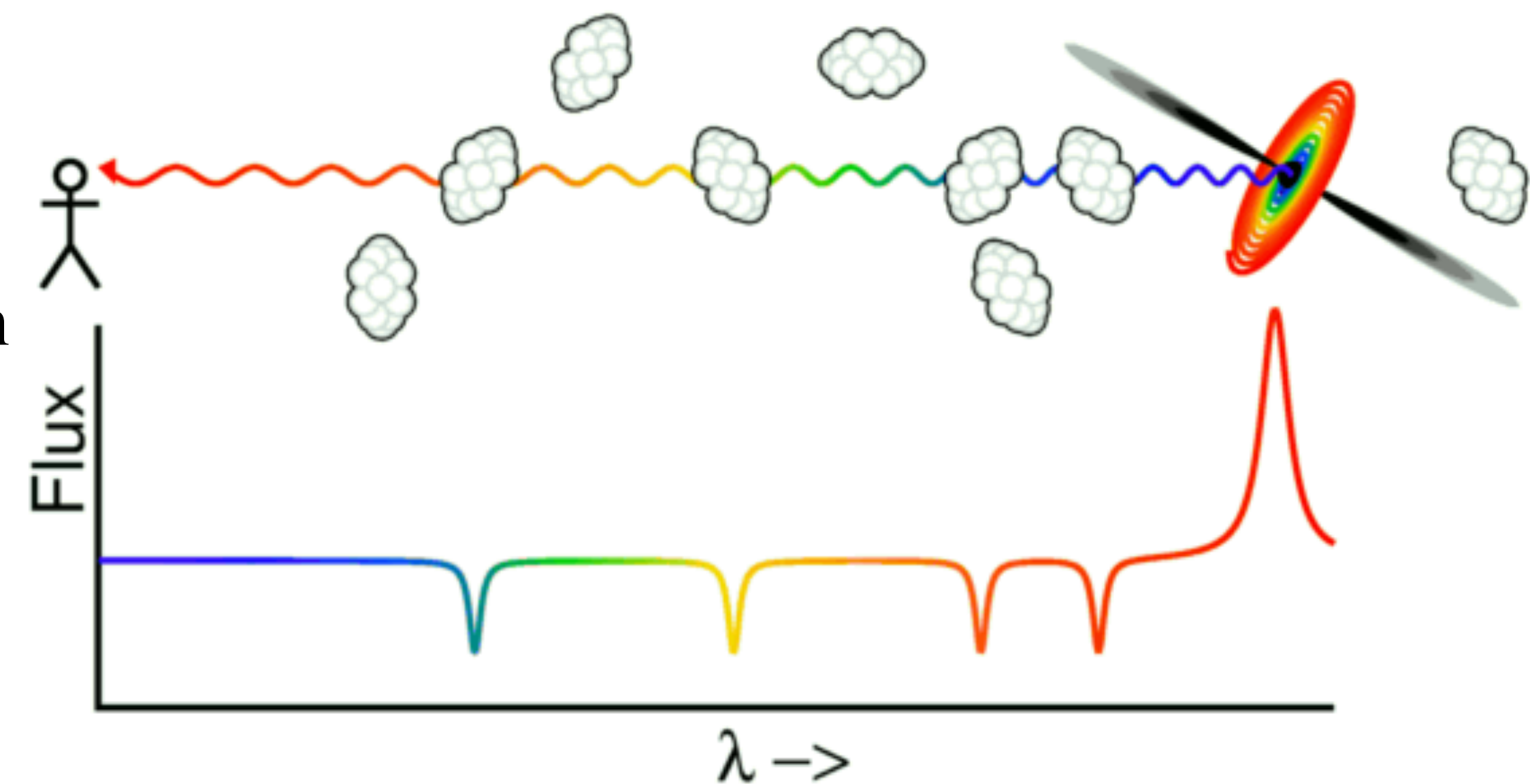
Absorption lines may also be present in some quasar spectra.

In particular, **Doppler-broadened absorption lines**, found in up to 10% of the spectra of quasars, originate from sources with **speeds exceeding 10^4 km s^{-1}** . These lines are believed to be **associated with the quasar itself**.

Many additional **narrow absorption lines** are typically seen in the spectra of quasars with high redshifts ($z > 2.2$) due to the **Lyman series of hydrogen** and metals such as **C IV and Mg II**.

These lines would normally appear at ultraviolet wavelengths but have been **redshifted into the visible spectrum** by the recessional velocity of the absorbing material.

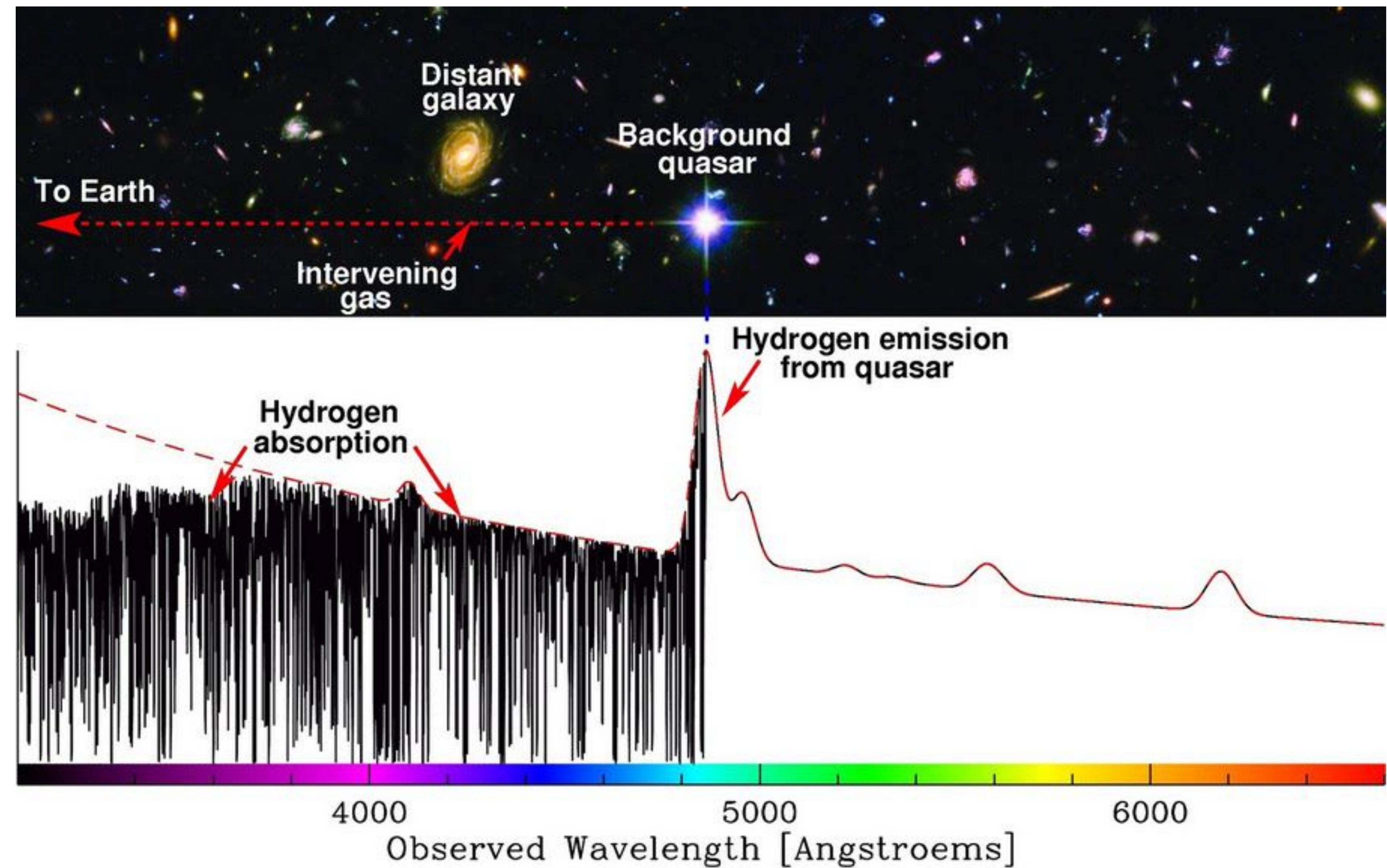
The absorption lines of a given quasar can be placed into **different groups that share common redshifts**. The various groupings of lines are thought to arise from **clouds of intervening material** that lie between the quasar and Earth.



Quasar spectra

The Lyman alpha forest:

In astronomical spectroscopy, the Lyman-alpha forest is a series of absorption lines in the spectra of distant galaxies and quasars arising from the Lyman-alpha electron transition of the neutral hydrogen atom. As the light travels through multiple gas clouds with different redshifts, multiple absorption lines are formed.



Quasi-Stellar Objects

The distinctive appearance of quasars, **starlike with an excess of ultraviolet light**, led astronomers to search for more objects fitting this description. In fact, choosing those objects with $U - B < -0.4$ (blue in colour) results in a nearly complete list of possible quasars (those at very high z are redder), which must then be confirmed by a spectroscopic analysis.

Researchers discovered that about 90% of the confirmed quasar candidates, and **AGNs in general, are relatively radio-quiet**. For this reason, most of these objects are technically referred to as **quasi-stellar objects** (QSOs), rather than quasars (QSRs). These objects tend to have very faint radio emission mostly only detectable through stacking.

Today, the term *quasar* has come to be used almost universally for both radio-loud QSRs and radio-quiet QSOs. As a result, it is common to encounter the descriptions **radio-loud quasars** and **radio-quiet quasars**. However, it is also sometimes the case that **QSO is used as an abbreviation for quasar**.

The terminology can be confusing in the literature.

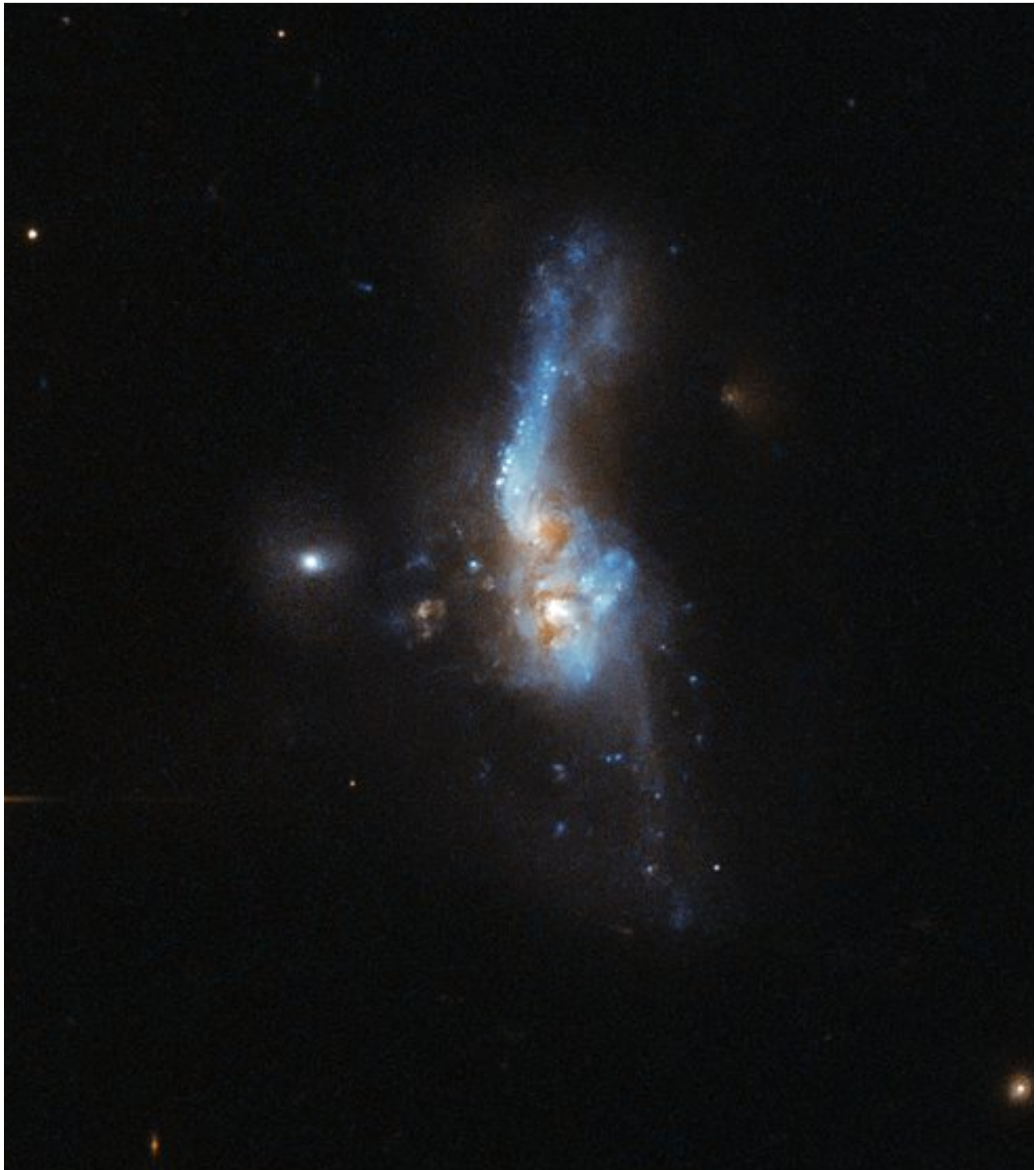
Ultraluminous inferred galaxies

Nearly all **quasars have spectra similar to those of broad-line radio galaxies and Seyfert 1s**, with bright power-law continua and broad emission lines.

Seyfert 2 spectra, with their narrow emission lines, appear to have no counterparts among the quasars. However, some astronomers argue that a subset of the galaxies that were cataloged by the IRAS satellite as being ultra-luminous at infrared wavelengths, known as **ultraluminous infrared galaxies (ULIRGs)**, should be **considered quasars of type 2** rather than **starburst galaxies**. It is suggested that the infrared light results from dust that absorbs and reradiates the light from the quasar nucleus.

According to one study a ULIRG is just part of an **evolutionary galaxy merger scenario**. In essence, two or more spiral galaxies, merge to form an early stage merger. After that, it becomes a late stage merger, which is a ULIRG. It then becomes a quasar and in the final stage of the evolution it becomes an elliptical galaxy.

IRAS 14348-1447 is an ultraluminous infrared galaxy, located over a billion light-years away.



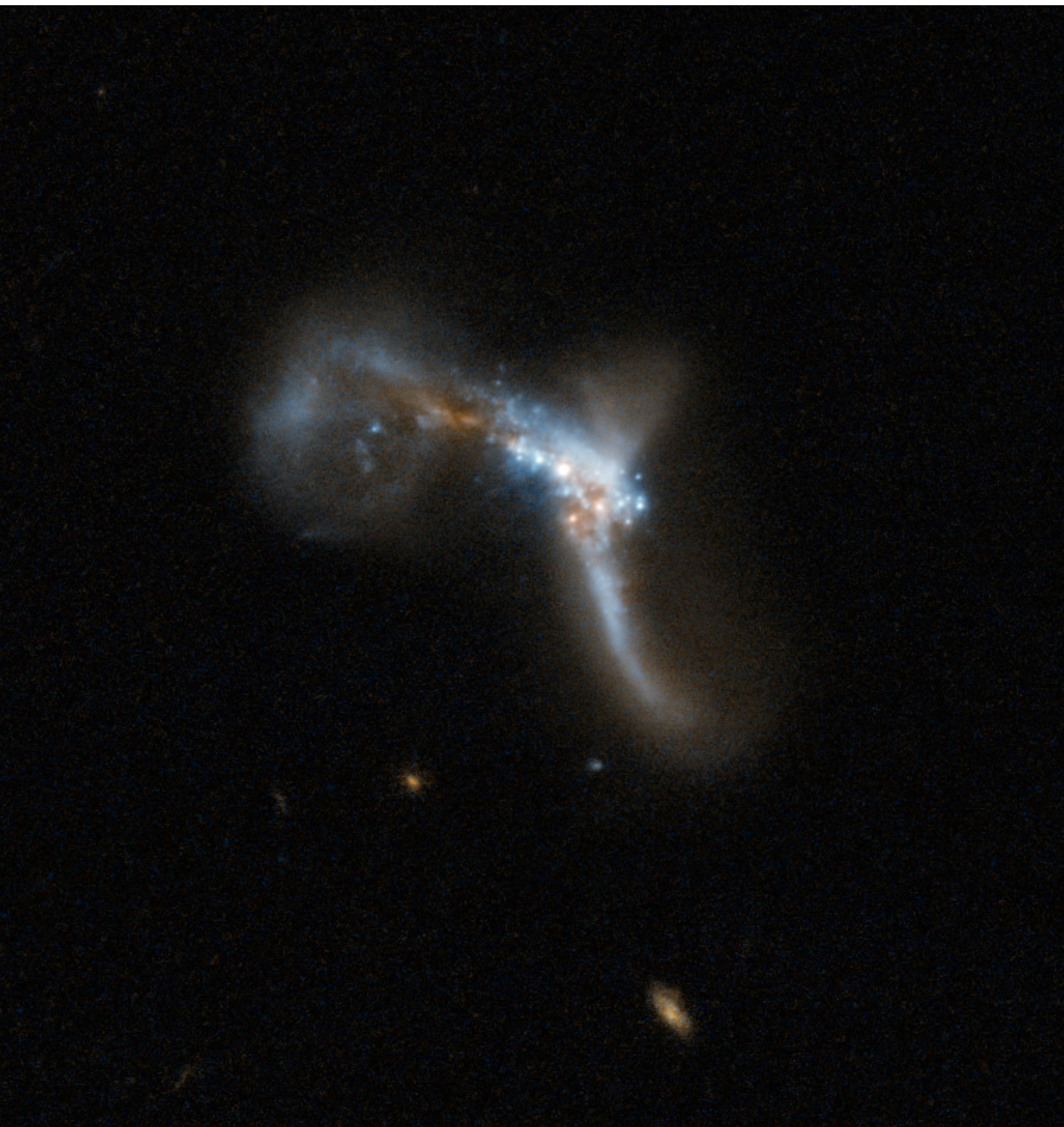
Ultraluminous inferred galaxies

The reason for this **intense infrared emission** lies in an **episode of strong star formation activity**, which was set off by a **collision** between two interacting galaxies.

In this image the twisted shape hides a number of features. In the central region, we can **distinguish two nuclei**, remains of the two different galaxies that are currently colliding.

IRAS 22491-1808 is amongst the most luminous of these types of galaxies, and is considered to be mid-way through its merging stage. The centre also shows several intense star-forming knots. Other traces of the galactic collision are the three very noticeable tails in the image — two linear and one circular.

IRAS 22491-1808, also known as the **South America Galaxy**. It is an ultraluminous infrared galaxy (ULIRG)



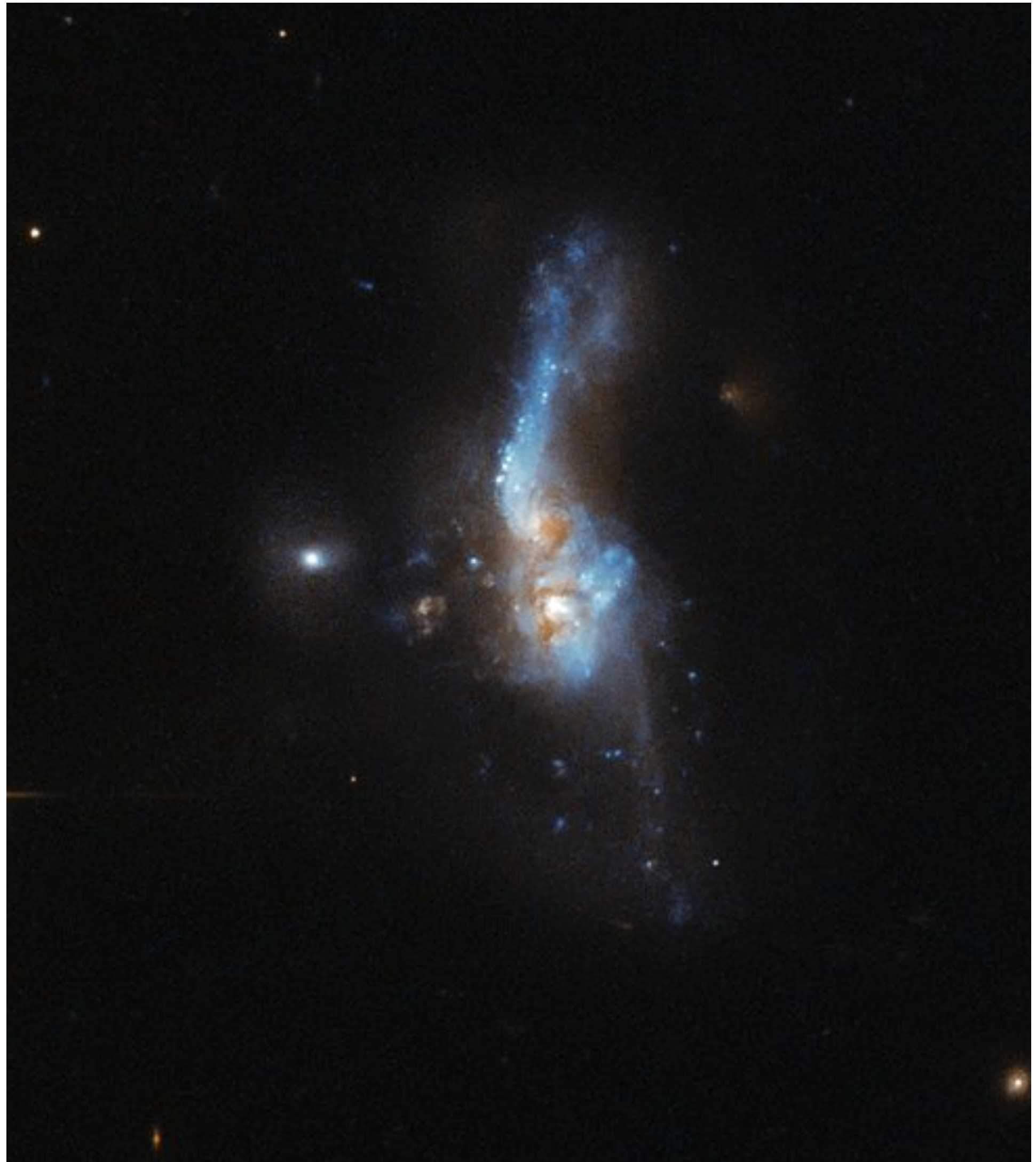
Ultraluminous inferred galaxies

Luminous infrared galaxies or LIRGs are **galaxies** with **luminosities**, the measurement of brightness, above $10^{11} L_\odot$. They are also referred to as **submillimeter galaxies (SMGs)**.

- Galaxies with luminosities above $10^{12} L_\odot$ are ultraluminous infrared galaxies (ULIRGs).
- Galaxies exceeding $10^{13} L_\odot$ are hyper-luminous infrared galaxies (HyLIRGs).
- Those exceeding $10^{14} L_\odot$ are extremely luminous infrared galaxies (ELIRGs).

Many of the LIRGs and ULIRGs are showing **interactions, disruptions and intense star formation**.

IRAS 14348-1447 is an ultraluminous infrared galaxy, located over a billion light-years away.



High redshift

The **Sloan Digital Sky Survey** (SDSS) has cataloged 46,420 quasars.

The brightest entry in the catalog in the i band (centered on a wavelength of 748.1 nm) is the object SDSS 17100.62+641209.0 at a redshift of $z = 2.7356$, having $M_i = -30.242$.

The most distant quasar in the catalog is SDSS 023137.65–072854.4 at a redshift of $z = 5.4135$, implying a recessional velocity of more than $0.95c$. In fact, there are 520 quasars in the SDSS catalog with redshifts greater than $z = 4$.

For such large cosmological redshifts, we must abandon using the Hubble law to determine distances.

Cosmological redshifts are caused by the expansion of the space through which the light travels, so for extremely large distances the total elongation of the wavelength depends on how the expansion of the universe has changed with time. The rate of expansion is changing in response to all of the matter and energy in the universe.

For this reason, it is customary to quote the redshift, z , rather than an actual distance determination.

High redshift

You should keep in mind, however, that the fractional change in wavelength for a cosmological redshift is the same as the fractional change in the size of the universe, R , since the time when the light was emitted.

$$z = \frac{\lambda_{\text{obs}} - \lambda_{\text{emitted}}}{\lambda_{\text{emitted}}} = \frac{R_{\text{obs}} - R_{\text{emitted}}}{R_{\text{emitted}}},$$

which gives

$$\frac{R_{\text{obs}}}{R_{\text{emitted}}} = 1 + z.$$

Thus a redshift of $z = 3$ means that the universe is now four times larger than when the light was emitted.